

Pseudopotential theory of interacting roton pairs in superfluid  $^4\text{He}$ 

K. Bedell

*Department of Physics, University of Illinois at Urbana—Champaign, Urbana, Illinois 61801  
and Department of Physics,\* State University of New York at Stony Brook, Stony Brook, New York 11794*D. Pines and A. Zawadowski<sup>†</sup>*Department of Physics, University of Illinois at Urbana—Champaign, Urbana, Illinois 61801*

(Received 28 June 1983)

A configuration-space pseudopotential, which is closely related to that used by Aldrich and Pines to describe the effective interaction between background particles in  $^3\text{He}$  and  $^4\text{He}$ , is constructed and used to calculate the roton-roton scattering amplitude. From that amplitude we obtain a theory that is completely congruent with the roton-liquid theory of Bedell, Pines, and Fomin. We calculate two-roton bound states, roton-liquid parameters, and roton lifetimes, as well as information about the hybridization of the two-roton bound state with excitations of higher and lower energy. Excellent agreement between theory and experiment is obtained for the  $l=2$  bound state at zero pair momentum, the roton lifetime, the roton contribution to the normal-fluid viscosity and the normal-fluid density, and the temperature variation of the roton energy. The effective roton-roton coupling parameters at large pair momentum are found to be an order of magnitude larger than those for small or vanishing pair momentum. At SVP we find that a substantial number of two-roton bound states of varying symmetry exist for pair momentum up to  $\sim 3 \text{ \AA}^{-1}$ ; at standard pressure, however the roton-roton interaction for momenta  $\sim 1 \text{ \AA}^{-1}$  is found to become repulsive, so that both the  $l=2$  bound state at zero pair momentum and bound states at intermediate momenta are predicted to disappear under pressure.

## I. INTRODUCTION

Since Landau<sup>1</sup> proposed the phonon-roton spectrum to explain the thermodynamical properties of superfluid  $^4\text{He}$ , great effort has been made to provide a microscopic derivation of that spectrum. After the pioneering work of Feynman and Cohen<sup>2,3</sup> the proposed excitation spectrum was verified by neutron scattering measurements.<sup>4-6</sup> More precise neutron scattering experiments revealed many new details (see Fig. 1), such as

- (i) the existence of a second branch of the excitation spectrum, located at higher energies than the phonon-roton branch, and
- (ii) saturation of the spectrum for large momenta at about  $2\Delta$ , where  $\Delta$  is the roton energy.

For wave vectors less than approximately  $2 \text{ \AA}^{-1}$ , the lower branch may be thought of as corresponding to the excitation of a single quasiparticle from the condensate, while the upper branch corresponds to exciting two or more quasiparticles from the condensate.<sup>4-6</sup> The saturation of the lower branch at momenta  $\sim 3 \text{ \AA}^{-1}$  was explained by Pitaevskii<sup>7</sup> as resulting from roton-roton scattering.

Following the discovery by Greytak and Yan<sup>8</sup> in a Raman scattering experiment of structure in the vicinity of  $2\Delta$ , Ruvalds and Zawadowski,<sup>9</sup> and independently Iwamoto,<sup>10</sup> suggested that the roton-roton interaction was attractive and that this attraction would lead to a two-roton resonance or bound state, which could explain the Raman

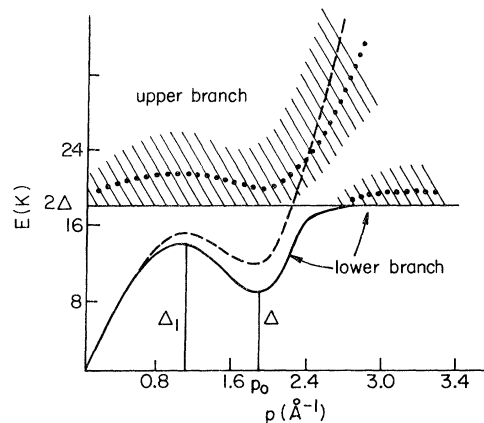


FIG. 1. Schematic depiction of the observed excitation spectrum of superfluid  $^4\text{He}$ . The spectrum suggested by Landau is shown by the dotted line. The hybridization between the two-roton branch with approximate energy  $2\Delta$  and Landau's spectrum results in two branches. The lower branch starts at  $E(K=0)=0$  and is shown by the solid line. At larger momenta the solid line merges into the shadowed area characteristic of the roton pairs. The upper multiparticle branch has the two-roton nature at smaller momenta, but around the hybridization point changes its character in such a way that its mean energy approaches the free particle energy  $q^2/2m$  with a breadth which is a considerable fraction of its mean energy. The shadowed region represents the range in energy of the multiparticle branch. The position of the center weights of the shadowed areas are indicated by points. The energy is shown on temperature scale.

scattering experiments of Greytak and his collaborators,<sup>8,11</sup> as well as making a significant contribution to the two excitation branches observed in neutron scattering experiments.<sup>9,10,12</sup> They further argued that hybridization of the two-roton resonant or bound states at momenta  $\sim 2.5 \text{ \AA}^{-1}$  with excitations that lie at higher and lower energies plays a significant role in determining the results of the neutron scattering experiments.

Our principal aim in this paper is to develop a theory which is capable of describing these and other major consequences of roton-roton interaction. These include the following:

- (1) The existence and binding energy of two-roton bound states as a function of roton pair momentum.
- (2) The temperature dependence of the roton energy and lifetime, which Mezei,<sup>13</sup> using spin-echo neutron scattering techniques, has determined to a high degree of accuracy and which are determined by roton-roton interactions at  $T \gtrsim 1.0 \text{ K}$ .
- (3) The temperature dependence of the normal fluid density  $\rho_n$ , at  $T \gtrsim 1.4 \text{ K}$ .
- (4) Transport coefficients of  $^4\text{He}$  in the temperature region ( $T \gtrsim 1.4 \text{ K}$ ) in which roton interactions play a dominant role.
- (5) The phenomenological parameters of the roton-liquid theory developed by Bedell, Pines, and Fomin<sup>14</sup> as a Bose-liquid analog of Landau's theory of Fermi liquids.
- (6) Neutron scattering experiments at momenta greater than approximately  $2.5 \text{ \AA}^{-1}$ .

There is some redundancy in this list, in that for  $1.4 \lesssim T \lesssim 1.8 \text{ K}$ , the viscosity and thermal conductivity are determined by the roton lifetime and energy, while the temperature dependence of the roton energy and the normal density are determined by the two lowest-order phenomenological parameters of roton-liquid theory.

Our basic approach is to describe roton-roton interaction by a pseudopotential that is closely related to that introduced by Aldrich and Pines<sup>15,16</sup> in their polarization-potential approach to the calculation of the phonon-maxon-roton branch of  $^4\text{He}$  and the density- and spin-fluctuation excitation spectra of  $^3\text{He}$ .<sup>16-18</sup> Aldrich and Pines have shown that the density-fluctuation excitations in  $^3\text{He}$  and  $^4\text{He}$  have a common origin in the force on a given quasiparticle arising from the average self-consistent fields of the other particles, and that this restoring force can be calculated from a configuration-space pseudopotential that has the following properties:

- (i) It is repulsive for  $r < r_c$ , attractive beyond.
- (ii) The attractive part of the interaction is identical to that for bare  $^4\text{He}$  atoms.
- (iii) The repulsive part is a soft-core interaction, whose strength at the origin,  $a$ , can be determined from the known spatial average of the pseudopotential.

We argue that since rotons are essentially excited  $^4\text{He}$  quasiparticles, their interaction should be describable by a similar kind of pseudopotential.

Our pseudopotential thus has only two adjustable parameters; these are chosen to obtain a fit to the experimentally determined binding energy in the  $l=2$  channel of roton pairs of net momentum zero, and the  $l=0$  interaction parameter of roton-liquid theory. Both the pseudopotential and the resulting scattering amplitude are found to possess a great deal of structure, a requirement which had been anticipated in the pioneering calculations of Fomin and Tüttö.<sup>12</sup> We use our two-roton scattering amplitude to calculate the aforementioned consequences of roton-roton interaction, with results which are in excellent agreement with experiment.

The paper is organized as follows: In Sec. II we give a brief review of theoretical and experimental work on two-roton states; because no recent review article on these states is available, we consider in some detail the interplay between bound states and the scattering amplitude, as well as between Raman scattering and neutron scattering experiments. Section III and the Appendix are devoted to the formal machinery required to calculate, via the scattering amplitude, the physical consequences of a given roton-roton pseudopotential. In Sec. IV we discuss the extent to which parameters that fix the roton-roton pseudopotential may vary, and we give the "best-fit" values for that interaction at saturated vapor pressure (SVP). In Sec. V we use the pseudopotential to calculate the two-roton bound-state energies as a function of pair momentum for various angular momentum channels, the roton-liquid parameters, and the roton lifetime; we also give our results for the way in which the pseudopotential and properties of the two-roton states vary with pressure. In Sec. VI the role of the two-roton spectrum in the neutron scattering is discussed briefly, and in Sec. VII we give our concluding remarks. The Appendix is devoted to the computational details related to the vertex functions.

## II. SURVEY OF EXPERIMENTS AND THEORIES CONCERNING TWO-ROTON STATES

The importance of the roton-roton scattering was first pointed out by Landau and Khalatnikov<sup>19</sup> who showed that it provides an explanation of the temperature-independent part of the viscosity of liquid  $^4\text{He}$  observed above  $\sim 1.4 \text{ K}$ . Here the dominant thermal excitations are the rotons; since their lifetime  $\tau$  is determined by roton-roton scattering, it is inversely proportional to the density of thermal rotons. Hence the roton contribution to the viscosity, which involves the product of that density and  $\tau$ , is independent of the temperature. Landau and Khalatnikov used the Born approximation to predict the strength of the roton-roton scattering from the experimental value of the viscosity.

Ten years later, Pitaevskii<sup>7</sup> showed that roton-roton scattering could explain the saturation of the lower branch of the excitation spectrum at large momenta, which had been established by neutron scattering experiments.<sup>4,5</sup> He further showed that if the roton-roton coupling were repulsive, there would be an end point of the spectrum at some critical value of the momentum and at energy  $2\Delta$ .

The first direct measurement on the two-roton spectrum was performed by Greytak and Yan,<sup>8</sup> who used Ra-

man scattering to study the excitation spectrum of  $^4\text{He}$ .<sup>11</sup> Under these circumstances the total momentum  $K$  of the excited roton pair is almost zero. The shape of the observed spectrum shows a strong deviation from the spectrum of two noninteracting rotors. Ruvalds and Zawadowski<sup>9</sup> and, independently, Iwamoto<sup>10</sup> suggested that the anomalous line shape is due to an attractive roton-roton interaction, which leads to the formation of a bound or resonant state with an energy just below the threshold of the two-roton continuum. Subsequently the resolution of the Raman scattering measurements was substantially improved,<sup>11</sup> while neutron scattering experiments made possible a more accurate determination of the roton energy  $\Delta(T)$ .<sup>20</sup> These experiments provide definitive evidence that the roton-roton interaction is attractive for small total momentum, and a two-roton resonance is formed below the two-roton energy.<sup>6</sup>

On the basis of the dipole character of the light scattering mechanism suggested by Stephens,<sup>21</sup> one can easily show that the roton pairs that are created must have angular momentum  $l=2$ . These pairs are not stable because (i) single rotors possess a lifetime which is strongly temperature dependent and (ii) a roton pair may directly decay into a phonon pair with the same energy, leading to a lifetime which is almost independent of the temperature.<sup>22</sup> At higher temperatures, the first mechanism is the dominant one; therefore, Raman scattering data combined with a theoretical expression for the line shape provides an accurate determination of the single-roton lifetime. The experimental results thereby obtained are in excellent agreement with the neutron scattering data of Mezei.<sup>13</sup> The comparison breaks down at lower temperatures as the second mechanism becomes dominant. From his experimental data, Mezei<sup>13</sup> obtained the following expression for the temperature dependence of the inverse lifetime and of the roton energy at SVP:

$$\frac{1}{2\tau_r(T)} = 47\sqrt{T} \exp\left[-\frac{\Delta(T)}{T}\right], \quad (2.1)$$

$$\Delta(T) - \Delta(0) = -19\sqrt{T} \exp\left[-\frac{\Delta(T)}{T}\right], \quad (2.2)$$

where all the quantities are given in units of K and at SVP.

What do these experiments tell us about the roton-roton interaction? First, as noted above light scattering provides information about the interaction in the limit of very small roton pair momenta  $K \sim 0$  and in the  $l=2$  channel. On the other hand, the roton lifetime is mostly influenced by pairs of momentum  $K \sim 1.5p_0$ .<sup>23</sup> Yau and Stephens<sup>22</sup> pointed out that a local (structureless) roton-roton interaction leads to a single-roton decay rate which is only about  $\frac{1}{4}$  of that observed. Similar conclusions have been drawn for the decay rate of the roton pairs which form the two-roton resonance.<sup>23</sup> [In this case, the rotors are not on energy shell, so that the imaginary self-energy  $\text{Im}\Sigma(\omega)$ , with off-energy-shell values of  $\omega$ , plays a role.] This failure to explain experiment indicates that the strength of roton-roton scattering estimated by Landau and Khalatnikov<sup>19</sup> is too strong for the Born approximation to be applicable.

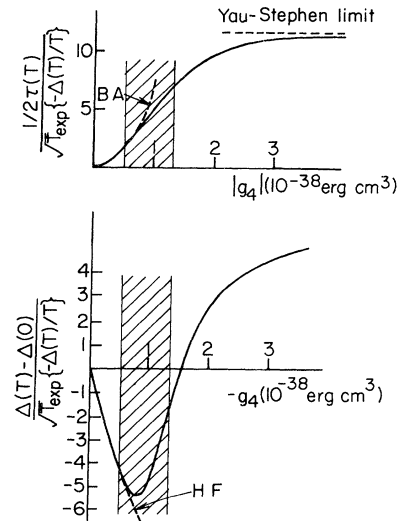


FIG. 2. Dependence of roton lifetime  $\tau(T)$  and the temperature shift of the roton energy  $\Delta(T) - \Delta(0)$  are shown as functions of the attractive roton-roton coupling strength  $g_4 < 0$ . Both quantities are normalized by the temperature-dependent factor  $\sqrt{T} \exp[-\Delta(T)/T]$ , which is proportional to the thermal density of rotors. The dotted lines indicate the results of Born approximation (BA) and Hartree-Fock approximation (HF), respectively. The normalized inverse lifetime  $T^{-1}(T)$  saturates at large coupling as pointed out by Yau and Stephens (Ref. 22). The energy shift measured is negative; thus only with  $|g_4| < 1.5 \times 10^{-38} \text{ erg cm}^3$  is one able to get the correct sign of the energy shift. Considering both quantities, the maximum available values are  $\frac{1}{4}$  of the experimental ones [see Eqs. (2.1) and (2.2)]. Thus several scattering channels are required to describe the experimental values. If a channel contributes to both quantities in an essential way, then the coupling strength must be in the shadowed areas. (Note that the coupling  $\Gamma_m$  used in the paper is  $\Gamma_m = 2g_4$ .) The curves have been calculated by Tüttő (Ref. 24).

A similar situation arises with the temperature-dependent shift of the roton energy  $\Delta(T)$ ,<sup>24,25</sup> which, like the roton lifetime, depends upon the roton-roton scattering amplitude. When one goes beyond the Born approximation to calculate this scattering amplitude, and then attempts to fit the roton lifetime and energy shift, one finds that no matter what coupling strength one assumes for a contact (local) interaction, one cannot obtain a fit to experiment.<sup>24</sup> This situation is illustrated in Fig. 2 which we take from the work of Tüttő.<sup>24</sup> The lessons of Fig. 2 are thus twofold:

- (1) It is not sufficient to use the Born approximation to calculate the roton-roton scattering amplitude.
- (2) In calculations of the scattering amplitude that go beyond the Born approximation, it is essential to work with a nonlocal roton-roton interaction.

We further note that the roton energy shift is negative, as is required by experiment, only in a narrow range of coupling strength.

These considerations led Fomin and Pitaevskii<sup>26,27</sup> to examine the conditions imposed by experiment on the structure of the roton-roton interaction. The symmetry of a roton pair depends upon the pair momentum  $\vec{K}$ . At  $\vec{K}=\vec{0}$  there is an exact rotational invariance in momentum space. At finite  $\vec{K}$ , the only exact symmetry is rotation about the axis of  $\vec{K}$ . Therefore for  $K=0$ , the total angular momentum  $l$  is a good quantum number; it must be even because of Bose statistics. At small pair momentum,  $K \ll p_0$ , the rotational invariance is weakly broken; thus the  $(2l+1)$ -fold degeneracy is split, and the states can be characterized by the azimuthal quantum numbers  $m=0, m=\pm 1, m=\pm 2, \dots, m=\pm l$ , where the relevant axis is parallel to  $\vec{K}$ . For large pair momenta ( $K \gtrsim p_0$ ), a different symmetry emerges. Consider a roton pair with momenta on or near the roton sphere of radius  $p_0$  as shown in Fig. 3. In roton-roton scattering, this pair ( $\vec{p}_1, \vec{p}_2$ ), whose momenta are inclined at some angle  $\theta$ , is scattered to another pair ( $\vec{p}_3, \vec{p}_4$ ) state; as long as the latter pair are also on or near the roton sphere, the angle between  $\vec{p}_3$  and  $\vec{p}_4$  is approximately also given by  $\theta$ . In addition to the angle  $\theta$ , each pair may be characterized by an azimuthal angle  $\phi$ , the angle between the projection on the plane perpendicular to  $\vec{K}$ , momentum of one of the rotons, and some axis in that plane (see Fig. 3). The symmetry of the wave function with respect to its dependence on  $\phi$  can be characterized by an azimuthal quantum number  $m$  again. The Bose character of rotons is reflected in the dependence on  $\phi$  in the wave function, if one assumes that the dependence of the pair wave function on the absolute value of the single-roton momentum  $p_1$  is smooth and that it does not have a zero near the roton sphere. For the roton pairs which are of physical interest,  $m$  takes only even values, as first shown by Fomin.<sup>26</sup> The scattering can then be described in terms of the scattering angle  $\Phi$  between the two planes determined by the momenta of the roton pairs before and after the scattering, respectively (see Fig. 4). In the crossover region between small  $\vec{K}$  and

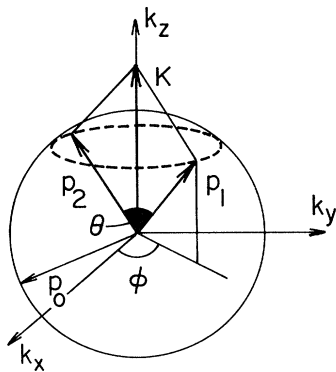


FIG. 3. Momenta  $\vec{p}_1$  and  $\vec{p}_2$  of a roton pair with total momentum  $K$  are shown. The momenta  $\vec{p}_1$  and  $\vec{p}_2$  are near the roton sphere. The possible positions of the momenta are indicated by the dotted circle. The angle between the momenta is denoted by  $\theta$ . The wave function of the pair with total momentum  $K$  depends on the angle  $\phi$  and the absolute values of momenta  $\vec{p}_1$  and  $\vec{p}_2$ .

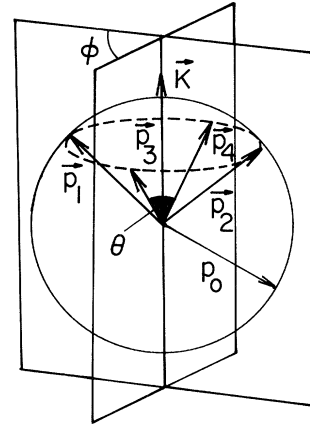


FIG. 4. Momentum space description of the scattering of a roton pair ( $\vec{p}_1, \vec{p}_2$ ) into another pair ( $\vec{p}_3, \vec{p}_4$ ). The total pair momentum  $K$  is conserved. The angle  $\phi$  between the planes formed by the momenta before and after the scattering is shown.

$K \sim p_0$ , the roton-pair wave functions possess no additional symmetry; the description of roton-roton scattering is rather complex, and one finds both odd and even values of  $m$  appearing.

Following Pitaevskii and Fomin,<sup>27</sup> the possible momentum dependence of bound states is illustrated in Fig. 5, where at small momenta two bound states are depicted with  $l=2,4$  with splitting according to  $m$ ; furthermore, at large momenta there is not more than one bound state for each even  $m$ . Finally, the intermediate region is extrapolated. It is important to point out, however, that bound states with the same  $m$  cannot intersect; thus for a given  $m$  only the lowest lying bound state at  $K \sim 0$  can continue to the larger momentum region. The different scattering

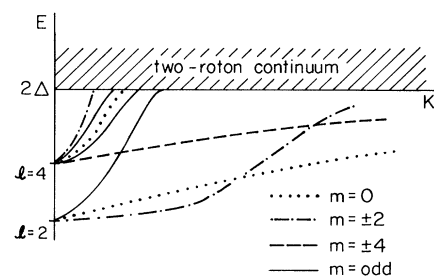


FIG. 5. Schematic depiction of the momentum dependence of the different two-roton bound-state energies, following Pitaevskii and Fomin (Ref. 27). At momentum  $K=0$  the bound states are characterized by the total angular momentum ( $l$  even). At finite momentum  $K$  the degeneracy is split. In the large momentum region the bound state is labeled by a single azimuthal quantum number ( $m$  even). The dispersion curves with different  $|m|$  are indicated by different lines given in the figure. The dispersion of the bound states with  $m$  odd starts at  $K=0$  and at larger momenta those quickly merge into the two-roton continuum. The curves shown are schematic; the angular momenta  $l=2,4$  are chosen as an example. It is important, however, to note that the dispersion curves with the same symmetry cannot cross.

channels characterized by  $m = 0, \pm 2, \pm 4, \dots$  contribute independently<sup>24,26</sup> to the lifetime and temperature-dependent energy shift of the rotons. Considering the shadow region in Fig. 2, the conclusion can be drawn that at least seven channels are required to explain the experimental data given by Eqs. (2.1) and (2.2). Thus the coupling strengths must be in the narrow shadowed interval shown in Fig. 2 if only seven channels contribute.

Additional information about the roton-roton interaction comes from neutron scattering experiments.<sup>28</sup> Neutron scattering is the only experimental technique which provides direct information about roton pairs of comparatively large net momentum,  $\vec{K}$ . Since only  $s$ -wave scattering of neutrons by the nuclei of the  $^4\text{He}$  atoms plays a significant role, that information is restricted to the  $m = 0$  channel of the roton-roton interaction. (Put another way, the excited roton pairs must be structureless in momentum space for rotations about their net momentum  $\vec{K}$ .) As Tüttö and Zawadowski<sup>29</sup> have emphasized, where hybridization of this two-roton state (with either the single-particle states which lie below it or the multiparticle states which lie above it) plays an important role, the effective roton-roton coupling constant in the  $m = 0$  channel can be significantly modified. As we discuss in further detail in Sec. VI, evidence that this is the correct physical picture comes from the fit to the neutron scattering data carried out by Smith *et al.*<sup>28</sup>

These results impose a number of constraints on the form of the roton-roton interaction. Previous theoretical attempts to obtain this interaction have tended to focus on comparatively isolated aspects of the consequences of the interaction (e.g., the  $l=0, l=2$  bound pair states at  $K=0$ ,<sup>30-34</sup> or the  $m=0$  states for large pair momentum<sup>34,35</sup>); to our knowledge there has been no prior attempt to pursue *all* the relevant consequences of the interaction, including of course, the existence of bound states at  $K=0$  with quantum numbers  $l \geq 4$ , and the momentum dependence of the  $m=0$  component of the interaction. For example, because the  $l=2$  bound state at  $K=0$  corresponds to an effective coupling that is weaker by almost an order of magnitude than those of higher angular momentum, theories that focus on deriving this energy from an effective weak attractive interaction, such as the phonon-induced interaction between rotons,<sup>33,36</sup> even though apparently successful, have obviously neglected the much larger attractive terms that are responsible for binding in  $l \geq 4$  states and for the observed lifetime and temperature-dependent energy of the rotons. (Thus we shall see in Sec. IV that this phonon-induced interaction is almost an order of magnitude smaller than the direct interaction we introduce there.)

Attempts have also been made to derive the effective roton-roton interaction from an equivalent weak coupling theory, in which the bare vertices are expressed in terms of the observed static structure factors, along the lines of the calculations of the excitation spectrum by Feenberg, Sunakawa, and their collaborators.<sup>37,38</sup> It has, however, proven difficult to get the resultant couplings to have the correct amplitudes and signs, as is evident from the results obtained from the most successful effort of this kind, that by Carballo and Ruvalds,<sup>30</sup> who took the effective interac-

tion to be a combination of a hard core and an attractive square well. A quite different approach has been taken by Roberts and Donnelly,<sup>39</sup> who adopt as a starting point a semiclassical treatment of roton interaction as that between classical point dipoles. While their numerical results are not far from experiment for some of the parameters they calculate, it appears difficult to connect their work with prior theoretical work, in which the starting point is a quantum treatment in terms of roton-roton scattering amplitudes.

In what follows, then, we shall attempt to be guided in our choice of a pseudopotential by both the need for considerable structure in the interaction and by the importance of being able to fit, at one and the same time, bound state and those aspects of the roton-roton interaction that are sensitive to interactions in higher momentum channels.

### III. SCATTERING AMPLITUDES, BOUND STATES, AND THE SELF-ENERGY FOR INTERACTING ROTONS

To establish the connection between our roton pseudopotential and experiment, we must study the roton-roton scattering amplitude and self-energy. Here we will be concerned with the contributions of the rotons to the transport, thermodynamics, etc., properties of superfluid  $^4\text{He}$ . The scattering states and bound states will involve energies that are much less than the roton energy  $\Delta$  and quasiparticle momenta that are close to the roton momentum  $p_0$ . The interaction between quasiparticles can then be viewed as scattering on a sphere of radius  $p_0$ , the roton sphere (see Figs. 3 and 4).

#### A. Bethe-Salpeter equation for the roton-roton scattering and the binding energies

In Fig. 6 we show the diagrammatic representation of the scattering amplitude; the scattering geometry is depicted in Fig. 4. As shown, e.g., by Fomin,<sup>26</sup> the Bethe-Salpeter equation for the symmetrized scattering amplitude  $\Gamma(\vec{k}, \vec{k}', \vec{K}, E)$  in the neighborhood of the roton minimum is given by

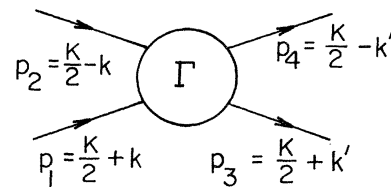


FIG. 6. Generalized two-roton-two-roton vertex  $\Gamma$ .  $\vec{K}$  is the total momentum of the roton pairs and  $\vec{k}$  ( $\vec{k}'$ ) is the relative momentum of the incoming (outgoing) rotons.

$$\Gamma(\vec{k}, \vec{k}'; \vec{K}, E) = \tilde{\Gamma}(\vec{k}, \vec{k}'; \vec{K}) + \frac{1}{2} \int \frac{d^3 k''}{(2\pi)^3} \tilde{\Gamma}(\vec{k}, \vec{k}'', \vec{K}) \left[ \frac{1}{E - \epsilon_{k''}^0 - \epsilon_{|\vec{K} - \vec{k}|} + i\delta} \right] \Gamma(\vec{k}'', \vec{k}'; \vec{K}, E) \quad (3.1)$$

with  $\vec{k} = \frac{1}{2}(\vec{p}_1 - \vec{p}_2)$ ,  $\vec{k}' = \frac{1}{2}(\vec{p}_3 - \vec{p}_4)$ , where  $\vec{K} = \vec{p}_1 + \vec{p}_2 = \vec{p}_3 + \vec{p}_4$ . The energy  $\epsilon_p^0$  is the experimental single-particle spectrum which is given by the Landau spectrum near  $p_0$ ,  $\epsilon_p^0 = \Delta_0 + (\vec{p} - \vec{p}_0)^2/2\mu$ , where  $\mu$  is the roton mass. The energy dependence of the irreducible symmetrized interaction  $\tilde{\Gamma}(\vec{k}, \vec{k}'; \vec{K})$  has been ignored in Eq. (3.1) since, if it exists at all, it will correspond to variations on an energy scale that is much larger than  $E - 2\Delta$ . All momenta  $\vec{p}_i$ ,  $i = 1-4$ , are assumed to lie on the roton sphere; hence the integral in Eq. (3.1) must be cut off. The choice for the cutoff momentum will be discussed later on.

### 1. Roton pair states with $K=0$

To study the two-roton bound states at zero total momentum we expand the interactions in a Legendre series in the scattering angle  $\theta_{kk'}$ , which is the angle between momenta  $k$  and  $k'$  (or  $p_1$  and  $p_3$ ). With all of the momenta on the roton sphere, both  $\tilde{\Gamma}(\vec{k}, \vec{k}'; \vec{K} = \vec{0})$  and  $\Gamma(\vec{k}, \vec{k}'; \vec{K} = \vec{0}, E)$  will depend only on the angle  $\theta_{kk'}$ ; thus

$$\tilde{\Gamma}(\vec{k}, \vec{k}'; \vec{K} = \vec{0}) = \sum_{l(\text{even})} (2l+1) \tilde{\Gamma}_l P_l(\cos\theta_{kk'}) \quad (3.2a)$$

$$\Gamma(\vec{k}, \vec{k}'; \vec{K} = \vec{0}, E) = \sum_{l(\text{even})} (2l+1) \Gamma_l(E) P_l(\cos\theta_{kk'}) \quad (3.2b)$$

Here we note that since rotons are bosons the interactions must be symmetric under exchange; thus only even partial waves will be present in Eqs. (3.2a) and (3.2b). If we now substitute Eqs. (3.2a) and (3.2b) into Eq. (3.1) and carry out the angular integrations we find

$$\Gamma_l(E) = \tilde{\Gamma}_l + \frac{1}{2} \int dk'' \frac{k''}{2\pi^2} \tilde{\Gamma}_l \frac{1}{E - 2\epsilon_{k''}^0 + i\delta} \Gamma_l(E) \quad (3.3)$$

where, after making the approximation  $k''^2 dk'' \approx p_0^2 dk''$ , we can ignore the need for a cutoff in momentum space, because any dependence of  $\Gamma_l$  on the cutoff will be weak.

For a bound state to exist,  $\tilde{\Gamma}_l$  must be attractive. When

$$\Gamma_m(K, E) = \tilde{\Gamma}_m(K) + \frac{1}{2K} \int_{p_0 - p_c}^{p_0 + p_c} dk'' \frac{k''}{2\pi} \int_{p_0 - p_c}^{p_0 + p_c} dp'' \frac{p''}{2\pi} \tilde{\Gamma}_m(K) \left[ \frac{1}{E - \epsilon_{k''}^0 - \epsilon_{p''}^0 + i\delta} \right] \Gamma_m(K, E) \quad (3.7)$$

where  $K = |\vec{K}|$  and  $p_c$  is a momentum cutoff. The energy denominator in Eq. (3.7) is given by

$$E - \epsilon_{k''}^0 - \epsilon_{p''}^0 = \xi - x^2 - y^2,$$

where  $\xi = E - 2\Delta_0$ ,  $x^2 = (\vec{k}'' - \vec{p}_0)^2/2\mu$ , and  $y^2 = (\vec{p}'' - \vec{p}_0)^2/2\mu$ .

To look for the possible bound states, with binding energy,  $\epsilon_m(K)$ , we can drop the imaginary part of the denominator (since  $E - \epsilon_{k''}^0 - \epsilon_{p''}^0 < 0$ ). The solution of Eq.

this happens the second term in Eq. (3.3) becomes much larger than the first; we can therefore drop the first term, and determine the binding energy  $\epsilon_l = 2\Delta - E$  for the  $l$ th channel from

$$\frac{1}{\tilde{\Gamma}_l} \approx -\frac{1}{2} p_0^2 \int_{-\infty}^{\infty} \frac{dk''}{2\pi^2} \left[ \frac{1}{\epsilon_l + (\vec{k}'' - \vec{p}_0)^2/\mu} \right] \quad (3.4)$$

The result is

$$\epsilon_l = \frac{p_0^2}{4\mu} \left[ \frac{\mu p_0}{2\pi} \tilde{\Gamma}_l \right]^2 \quad (3.5)$$

These results agree with the previous calculations (see Ref. 12, where the notation  $\tilde{\Gamma}^l = 2g^l$  is implied). Bound states of two rotons with relative angular momentum  $l=2$  have been observed by Greytak and Yan.<sup>8</sup>

### 2. Roton-pair states with $K \neq 0$

Let us turn to the Bethe-Salpeter equation (3.1) in the case of  $K \neq 0$ . The solutions we obtain will be used to calculate the self-energy and the bound states with  $K \neq 0$ .

For finite total momentum  $K$  we can obtain a solution for Eq. (3.1) by expanding the vertex in a Fourier series in  $\phi$ . (See Fig. 4 for definition of  $\phi$ .) With all momenta on the roton sphere, Eq. (3.1) reduces to a set of uncoupled integral equations for each  $m$  channel, where  $m$  is the projection of the angular momentum  $\vec{K}$ . Expanding the interactions on the roton sphere ( $p_i = p_0$  for  $i = 1-4$ ) in the azimuthal channels  $m$  we have

$$\tilde{\Gamma}(\vec{k}, \vec{k}'; \vec{K}) = \sum_{m(\text{even})} \tilde{\Gamma}_m(K) e^{im\phi} \quad (3.6a)$$

and

$$\Gamma(\vec{k}, \vec{k}'; \vec{K}, E) = \sum_{m(\text{even})} \Gamma_m(K, E) e^{im\phi} \quad (3.6b)$$

For finite  $\vec{K}$  we make a change of variables in Eq. (3.1), setting  $|\vec{p}''| = |\vec{K} - \vec{k}''|$ . By integrating over  $\phi$  we find an integral equation for each azimuthal channel,

(3.7) is then

$$\Gamma_m(K, E = 2\Delta_0 + \xi)$$

$$= \tilde{\Gamma}_m(K) / \left[ 1 + \frac{\mu p_0^2}{4\pi K} \tilde{\Gamma}_m(K) \ln \left[ \frac{2x_c^2}{\xi} \right] \right] \quad (3.8)$$

which, for the case of negative  $\tilde{\Gamma}_m(K)$ , yields a binding energy

$$\epsilon_m(K) = 2x_c^2 \exp \left[ - \left( \frac{\mu p_0^2}{4\pi K} \right)^{-1} \left| \tilde{\Gamma}_m(K) \right|^{-1} \right], \quad (3.9)$$

where we have taken into account that  $x_c^2 = p_c^2/2\mu \gg \epsilon_m(K)$ . This result likewise agrees with the previous calculations (see Ref. 12 and the note that  $\Gamma_m = 2g_4^m$ ).

### B. The roton self-energy

To determine  $\Delta(T)$  and  $\tau(T)$  we must calculate the roton self-energy  $\Sigma(p, \omega)$ . The real part of the self-energy evaluated at  $|\vec{p}| = p_0$  and  $\epsilon = \Delta$  will determine  $\Delta(T)$ . From the imaginary part we obtain  $\tau(T)$ , which also determines the roton contribution to the transport properties of superfluid  $^4\text{He}$ . Expressions for the roton self-energy have been derived by a number of authors,<sup>12,14,24-26</sup> who find that it can be expanded in the number of rotons, where to first order in the number of rotons we have

$$\Sigma(\vec{p}, \omega) = \int \frac{d^3 p'}{(2\pi)^3} \Gamma(\vec{p}, \vec{p}'; E = \omega + \epsilon_{\vec{p}}) n(\epsilon_{p'}), \quad (3.10)$$

where

$$n(\epsilon_p) = \frac{1}{e^{\epsilon_p/k_B T} - 1}$$

is the roton distribution function. The diagrammatic structure of Eq. (3.10) is shown in Fig. 7.

The scattering amplitude in Eq. (3.10) is the limit of  $\Gamma(\vec{k}, \vec{k}'; \vec{K}, E)$  in Eq. (3.1) with  $\vec{q} = \vec{p}_1 - \vec{p}_3 = \vec{p}_4 - \vec{p}_2 = \vec{0}$ . Here, for convenience, we have introduced the variables  $\vec{p} = \vec{p}_1 = \vec{p}_3$  and  $\vec{p}' = \vec{p}_2 = \vec{p}_4$  with  $\vec{K} = \vec{p} + \vec{p}'$ , so that the scattering angle  $\phi = 0$ ; thus  $\Gamma(\vec{p}, \vec{p}'; E) = \sum_m \Gamma_m(K, E)$  [see Eq. (3.6b)].

We now consider the choice of a cutoff and the energy dependence of  $\Gamma_m(\vec{K}, E)$ . An energy cutoff  $x_c^2 = p_c^2/2\mu$  is introduced in order to separate the integral into terms that are near  $p_0$  and far from  $p_0$ . A natural choice for this cutoff is to use the point at which the true quasiparticle spectrum deviates from the Landau spectrum  $\epsilon_p^0 = \Delta + (\vec{p} - \vec{p}_0)^2/2\mu$ . Experimentally this occurs at an energy which is approximately half-way between the roton momentum  $p_0$  and the maxon momentum  $p_1 \approx 1.1 \text{ \AA}^{-1}$ .

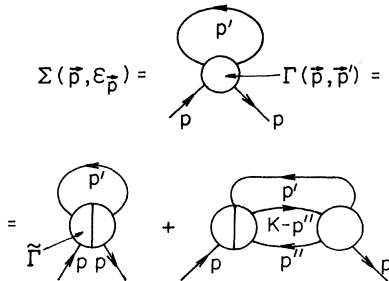


FIG. 7. Diagrammatic structure of the roton self-energy. The circle with the line through it is the irreducible roton-roton interaction.

This was the value used by Zawadowski *et al.*<sup>12</sup> in their study of bound states at finite  $K$ . The corresponding momentum cutoff is  $p_c/p_0 \approx 0.19$  at all pressures. This choice is consistent with experiment, since Dietrich *et al.*<sup>40</sup> find that at all pressures the Landau spectrum fits the experimental spectrum in the range  $|(\vec{p} - \vec{p}_0)/p_0| \leq 0.17$  to within 10% at the end points. The corresponding energy cutoff is approximately given by  $x_c^2 = \Delta - \Delta_1$  at all pressures, where  $\Delta_1$  is the maxon energy.

In order to calculate  $\Sigma(p, \omega)$  given by Eq. (3.10), we must solve the Bethe-Salpeter equation (3.7) for  $\xi > 0$ . It is straightforward to integrate Eq. (3.7) to obtain<sup>9,12,26</sup>

$$\Gamma_m(K, E = 2\Delta + \xi) = \frac{\tilde{\Gamma}_m(K)}{1 + \frac{\mu p_0^2}{4\pi K} \left[ i\pi + \ln \left( \frac{2x_c^2}{\xi} \right) \right]} \tilde{\Gamma}_m(K), \quad (3.11)$$

where  $x_c^2 = p_c^2/2\mu \gg \xi$  has been used. It should be noted that the solutions given by Eq. (3.11) are valid only for not very small  $K$  ( $K \gg 0.1p_0$ ).<sup>12</sup> However, the important region of  $K$  values is  $\frac{1}{2}p_0 < K \leq 2p_0$ ,<sup>23,24</sup> thus we can use Eq. (3.11) for all  $K$ .

We further note that in general  $\tilde{\Gamma}_{m=0}(K)$  must be corrected to take into account effects associated with hybridization.<sup>23,24</sup> Such corrections will be discussed in Sec. VI in the context of neutron scattering. Since these corrections exist only in the channel  $m=0$ , these will not affect our calculations for  $\Delta(T)$  and  $\tau(T)$  in an essential way.

The expression (3.10) for the self-energy can be further simplified if we make Fomin's approximation of replacing the energy variable  $E$  by  $\omega + k_B T$ . To justify this approximation, we note that in the integration over  $p'$  in Eq. (3.10) the important region is  $(\vec{p} - \vec{p}_0)^2/2\mu \sim k_B T$ . Fomin,<sup>26</sup> in his calculation of the transport properties of superfluid  $^4\text{He}$ , showed that the approximation introduces errors of the order  $\mu k_B T/p_0^2 \sim 1\%$  in the viscosity coefficient. In order to make the calculations still simpler a fixed typical value will be used for the temperature  $T$  in Eq. (3.10), such that throughout the temperature range  $\frac{1}{2}\Gamma_r(T) \ll T$ , where  $\Gamma_r(T)$  is the roton halfwidth, and  $\Delta_0 - \Delta(T) \ll T$ , where  $\Delta_0 = \Delta(T=0)$ . These conditions are consistent with the expansion to first order in the number of rotons used in Eq. (3.10). We choose this temperature as  $T \approx 1.4 \text{ K}$  and thus set  $\xi = 1.4 \text{ K}$  in our calculations for all pressures and all temperatures. The temperature dependence of  $\Delta(T)$  or  $\Gamma_r(T)$  will then come entirely from the number of rotons  $N_r(T)$ .

### C. Temperature dependence of $\Delta$

The energy  $\epsilon_p$  is defined as the pole of the single-particle Green's function,

$$\text{Re}G^{-1}(p, \epsilon_p) = \epsilon_p - [\epsilon_p^0 + \text{Re}\Sigma(p, \epsilon_p)] = 0. \quad (3.12)$$

In terms of the moments  $\Gamma_m(\vec{K}, E)$ , the temperature dependence of the roton energy  $\Delta$  takes a very simple

form. For  $\Delta(T)$  we evaluate Eq. (3.12) at  $|\vec{p}'|=p_0$ ; we find

$$\Delta(T) = \Delta_0 + f_0 N_r(T), \quad (3.13)$$

where

$$\begin{aligned} N_r(T) &= \int dp' \frac{p'^2}{2\pi^2} n(\epsilon_{p'}) \\ &= 2 \left[ \frac{\mu}{2\pi} \right]^{3/2} (1 + \alpha \sqrt{\mu T}) \frac{p_0^2}{\mu} \sqrt{T} \exp \left[ -\frac{\Delta(T)}{T} \right], \end{aligned} \quad (3.14)$$

where the constant  $\alpha = 0.525 \text{ \AA}$  takes into account the cubic corrections to the roton dispersion curve [see Eq. (20) in Ref. 14]. The parameter  $f_0$  is just the  $l=0$  moment of the roton interaction  $f_{\vec{p}\vec{p}'}$ , introduced by Bedell, Pines, and Fomin.<sup>14</sup> The expression for  $f_0$  in terms of  $\Gamma_m$  will be given at the end of this section.

#### D. Roton lifetime

The imaginary part of  $\Gamma_m(K, E)$  determines the roton lifetime, where

$$\begin{aligned} \frac{1}{2\tau(T)} &= -\text{Im}\Sigma(p_0, \epsilon_{p_0} + i\delta) \\ &= N_r(T) \int_{-1}^1 \frac{dx}{2} \sum_{m(\text{even})} \text{Im}\Gamma_m(K, E + i\delta), \end{aligned} \quad (3.15)$$

where  $x = (\vec{p} \cdot \vec{p}')/p_0^2$ . This can be connected with Fomin's<sup>26</sup> calculation of the viscosity by first noting that

$$\text{Im}\Gamma_m(K, E + i\delta) = -\frac{\mu p_0^2}{K} |\Gamma_m(K, E)|^2,$$

and

$$dx = \frac{K dK}{p_0^2},$$

so that

$$\frac{1}{2\tau(T)} = \frac{\mu p_0}{4} N_r(T) \bar{w}. \quad (3.16)$$

Here  $\bar{w}$  is the scattering rate defined by

$$\bar{w} = 2 \int_0^{2p_0} \frac{dK}{p_0} \sum_m |\Gamma_m(K, E)|^2,$$

which enters into the viscosity  $\eta$ ,<sup>26</sup>

$$\eta = \frac{2p_0}{15} \frac{1}{\mu^2} \bar{w}^{-1}, \quad (3.17)$$

with  $\hbar=1$ .

#### E. Connection with roton-liquid theory

The roton-liquid theory proposed by Bedell, Pines, and Fomin<sup>14</sup> is based on the idea that thermodynamics of rotons can be expressed by the roton number and by the re-

normalized vertex functions  $\Gamma_m$  taken at some characteristic energy value. We have seen in our calculation of the self-energy given by Eq. (3.10) that in taking the self-energy at fixed energy  $\omega = \Delta$  the energy dependence of the vertex function  $\Gamma_m$  can be ignored, provided one chooses the correct characteristic energy to evaluate  $\Gamma_m$ . The choice of the characteristic energy in principle depends on the temperature, but in the temperature range  $1.0 < T < 1.8$  K this dependence is sufficiently weak that one can take an average value  $T = 1.4$  K. This approximation is the basic ingredient of the roton-liquid theory, which then shows a strong resemblance to Landau's Fermi-liquid theory.

For completeness we give the expressions which relate the roton-liquid parameters of Bedell, Pines, and Fomin<sup>14</sup> to the renormalized scattering amplitudes  $\Gamma_m$  that we have obtained from the Bethe-Salpeter equation.

The roton-liquid vertex  $f_{\vec{p}\vec{p}'}$  and the diagonal value of the vertex  $\Gamma$  are related through

$$f_{\vec{p}\vec{p}'} = \text{Re}\Gamma(\vec{p}, \vec{p}'; E = 2\Delta + T), \quad (3.18)$$

where  $T$  is taken to be  $T = 1.4$  K [the vertex  $\Gamma(\vec{p}, \vec{p}'; E)$  is introduced in Eq. (3.10)]. Because all rotons are assumed to lie on the roton sphere,  $f_{\vec{p}\vec{p}'}$  may be expanded in Legendre polynomials as

$$f_{\vec{p}\vec{p}'} = \sum_l f_l P_l(x), \quad (3.19)$$

where  $f_l$  are the roton-liquid coefficients and  $x = (\vec{p} \cdot \vec{p}')/p_0^2$ , ( $|\vec{p}| = |\vec{p}'| = p_0$ ). Using Eq. (3.6b) for  $\Gamma_m$  in Eq. (3.18) and combining the inverse of Eq. (3.19) with Eq. (3.18), one gets

$$f_l = \frac{2l+1}{2} \int_{-1}^1 dx' P_l(x') \sum_{m(\text{even})} \text{Re}\Gamma_m(K, E), \quad (3.20)$$

where  $K^2 = 2p_0^2(1+x')$ .

#### IV. ROTON-ROTON PSEUDOPOTENTIAL

According to Aldrich and Pines,<sup>16</sup> a roton is an excited quasiparticle of momentum  $\sim p_0$ , effective mass  $\sim 2.1M$  ( $M$  is the mass of a bare  $^4\text{He}$  atom) moving in an attractive self-consistent field ( $\simeq -2$  K) produced by the other quasiparticles in the liquid. It seems natural therefore to attempt a configuration-space description of roton interaction,  $\tilde{f}(r)$ , which is similar to the configuration-space interaction devised by Aldrich and Pines<sup>16</sup> for the effective interaction between an excited  $^4\text{He}$  atom and one in the ground state, viz., a long-range interaction that is identical to that between bare  $^4\text{He}$  atoms, which becomes repulsive at some radius  $r_c$ ; as with the ground-state particles, we expect the short-range correlations brought about by the strong short-range repulsive part of the bare interaction will change the latter from its almost hard-core behavior to a soft-core repulsion, such that the overall potential possesses a well-defined Fourier transform. To the extent that the transition from attraction to repulsion occurs over a distance small compared to  $r_c$ , and the exact form of the repulsion is of little importance, this potential  $\tilde{f}(r)$  may be characterized by two parameters:  $r_c$  and  $a$ , the

strength of the repulsive interaction at the origin.

A second contribution to the roton-roton pseudopotential comes from the coupling of rotons to the  $^4\text{He}$  background particles, a process analogous to the phonon-induced interaction between electrons in a metal or that between  $^3\text{He}$  atoms in a dilute  $^3\text{He}$ - $^4\text{He}$  mixture. If we write the basic  $^4\text{He}$ -roton interaction as

$$\sum_q u_q \rho_{\vec{q}} a_{\vec{p}+\vec{q}}^\dagger a_{\vec{p}}, \quad (4.1)$$

where  $\rho_{\vec{q}}$  is a  $^4\text{He}$  density fluctuation excitation, and the operators  $a_{\vec{p}}$  and  $a_{\vec{p}+\vec{q}}^\dagger$  act to destroy a roton of momentum  $\vec{p}$ , create one of  $\vec{p}+\vec{q}$ , then to the extent that we confine our attention to low-frequency processes on or near the energy shell, the resulting induced interaction between rotons (depicted in Fig. 8) will take the form

$$V_{\text{ind}}(q) = \sum_q |u_q|^2 \chi(q, 0), \quad (4.2)$$

where  $\chi(q, 0)$  is the static wave-vector-dependent susceptibility of  $^4\text{He}$ . We use deformation-potential theory to obtain the long-wavelength form of  $u_q$ ,

$$\begin{aligned} \lim_{q \rightarrow 0} u_q(q) &= \frac{\partial \Delta}{\partial N} \simeq -\frac{\Delta}{N} \\ &= -\left[ \frac{ms^2}{N} \right] \left[ \frac{\Delta}{ms^2} \right] \end{aligned} \quad (4.3)$$

on making use of the appropriate experimental value,  $\partial \Delta / \partial \rho \simeq -\Delta / N$ .<sup>40</sup> Since  $\lim_{q \rightarrow 0} \chi(q, 0) = -N / ms^2$ , we find

$$\lim_{q \rightarrow 0} V_{\text{ind}}(q) \simeq -\frac{ms^2}{N} \left[ \frac{\Delta}{ms^2} \right]^2. \quad (4.4)$$

At SVP,  $NV_{\text{ind}}(0) \simeq -2.7$  K; it is still smaller ( $\sim -0.82$  K) at melting pressure. As we shall see below, these values are to be compared with the long-wavelength result for the direct interaction between rotons, which is

$$N \int d^3r \tilde{f}(r) = N \tilde{f}_0 \approx -25 \text{ K}$$

at all pressures. We therefore do not attempt to parametrize explicitly the phonon-roton induced interaction, (4.2), but instead take the view that in parametrizing the direct interaction,  $\tilde{f}(r)$ , we can include to sufficient accuracy any effects of the induced interaction.

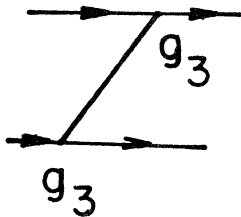


FIG. 8. Diagrammatic representation of that part of the roton-roton interaction,  $g_4$ , which is mediated by a single excitation.  $g_3$  indicates the interaction in which the roton emits or absorbs another excitation.

Given a model pseudopotential with Fourier transform

$$\tilde{f}_q = \int d^3r \tilde{f}(r) e^{i\vec{q} \cdot \vec{r}}, \quad (4.5)$$

we can calculate the irreducible symmetrized vertex,  $\tilde{\Gamma}(\vec{p}_1, \vec{p}_2; \vec{p}_3, \vec{p}_4)$ , defined through Eq. (3.1). Since rotons are bosons the irreducible interaction must be symmetric under exchange of the incoming or outgoing particles. Thus

$$\tilde{\Gamma}(\vec{p}_1, \vec{p}_2; \vec{p}_3, \vec{p}_4) = \tilde{f}_q + \tilde{f}_{q'}, \quad (4.6)$$

where  $\vec{q} = \vec{p}_1 - \vec{p}_3$  and  $\vec{q}' = \vec{p}_1 - \vec{p}_4$ .

In calculating  $\tilde{f}(r)$  and  $\tilde{f}_q$  we have used for the long-range part of  $\tilde{f}(r)$  ( $r \geq r_c$ ) a simple analytic potential which has been constructed to fit the potential of Aziz *et al.*<sup>41</sup> shown in Fig. 9 within 3% accuracy

$$V(r) = \begin{cases} a_1 \left[ \left( \frac{r_0}{r} \right)^{12} - \left( \frac{r_0}{r} \right)^6 \right], & r \leq 3.4 \\ -a_2 \left( \frac{r_0}{r} \right)^6, & r \geq 3.4 \end{cases}$$

( $r$  in units of  $\text{\AA}$ ) where,  $r_0 = 2.646$   $\text{\AA}$ ,  $a_1 = 42.98$  K, and  $a_2 = 33.4309$  K. This was chosen for its simplicity and ease in obtaining a Fourier transform. (For our calculations a more accurate potential is not needed.) For the repulsive part of the potential we use the same form of the potential as that adopted by Aldrich and Pines<sup>16</sup> for  $^3\text{He}$  and  $^4\text{He}$ ,

$$\tilde{f}(r) = a \left[ 1 - \left( \frac{r}{r_c} \right)^8 \right], \quad r \leq r_c.$$

At  $P = 0.0$  the parameters  $a$  and  $r_c$  of the pseudopotential

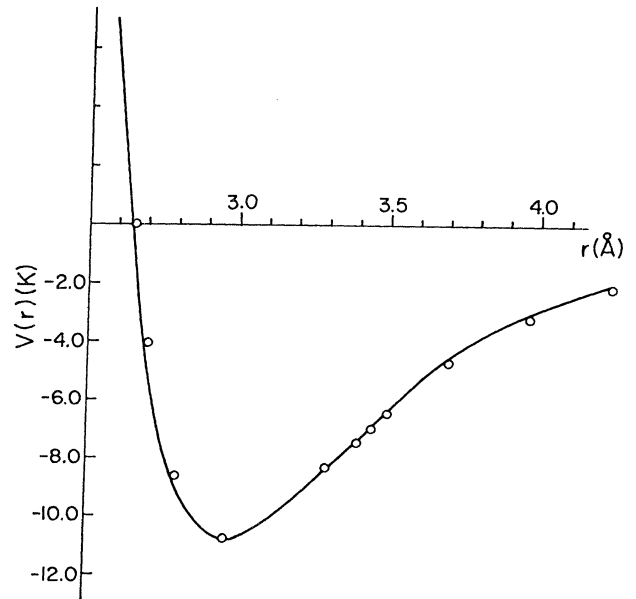


FIG. 9. Helium potential used in the calculation. The potential used was a fit to the Aziz potential (Ref. 41), values for the Aziz potential are shown as open circles. The fit is within a few percent for  $r > 2.8$   $\text{\AA}$ .

tial  $\tilde{f}(r)$  are chosen so as to yield the following.

(i) The experimentally determined binding energy<sup>42</sup> of the  $l=2$  bound state for  $K=0$ ,  $\epsilon_{l=2}=0.27\pm 0.04$  K.

(ii) The roton-liquid parameter  $f_0$  determined by Bedell, Pines, and Fomin<sup>14</sup> from fits to both specific heat measurements and neutron scattering experiments on the roton energy,  $Nf_0 = -9.7$  K.

In the course of choosing the best values of  $r_c$  and  $a$ , we found that binding in the  $l=2$  channel occurs for only a limited range of  $r_c$ ,

$$3.1 \lesssim r_c \lesssim 3.6$$

(in units of  $\text{\AA}$ ), no matter what the choice of  $a$ . Within this range of a given value of  $r_c$ , one can find a value of  $a$  which yields the  $l=2$  bound state. However, the requirement that one also obtain  $f_0$  in agreement with experiment uniquely determines both  $r_c$  and  $a$ . Our best fit to  $f_0$  was obtained with  $r_c = 3.3$   $\text{\AA}$  and  $a = 1.48$  K. If, instead, one takes  $r_c = 3.4$   $\text{\AA}$  and  $a = 1.48$  K, one finds a fit to the  $l=2$  bound state, but  $Nf_0$  is some 10% larger, being  $-10.7$  K. The potential  $\tilde{f}(r)$  and its Fourier transform  $\tilde{f}_q$  are shown in Figs. 10 and 11, respectively.

In the  $^3\text{He}$  and  $^4\text{He}$  systems it can be argued that the exact shape of the core used in Ref. 18 is not important since the momenta studied, up to  $2 \text{\AA}^{-1}$ , do not signifi-

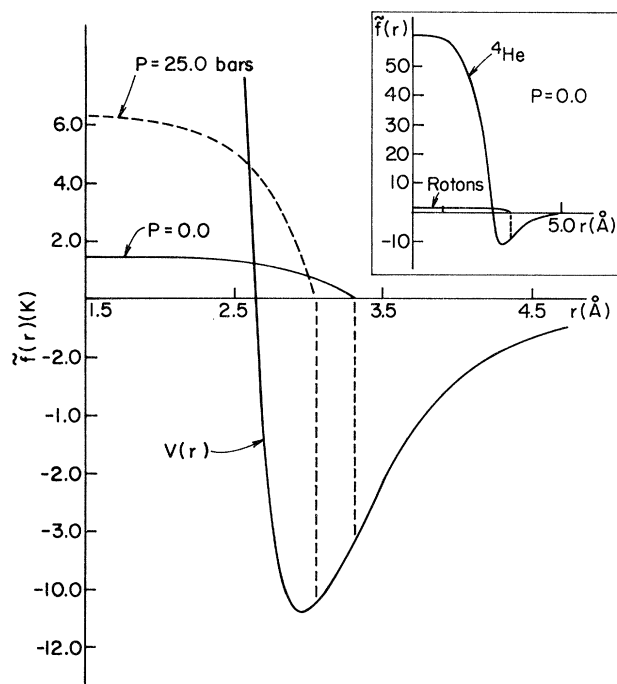


FIG. 10. Roton pseudopotential  $\tilde{f}(r)$  for two pressures  $p=0.0$  and  $p=25.0$  bars. The qualitative feature of decreasing core radius and increasing core height with increasing pressure is similar to that found in the  $^3\text{He}$  system.  $V(r)$  is the potential shown in Fig. 9. The inset is given to compare the roton-roton potential at  $p=0.0$  bar with the polarization potential ( $^4\text{He}$ ) proposed by Aldrich and Pines (Ref. 16) for the phonon-maxon-roton spectrum of  $^4\text{He}$ .

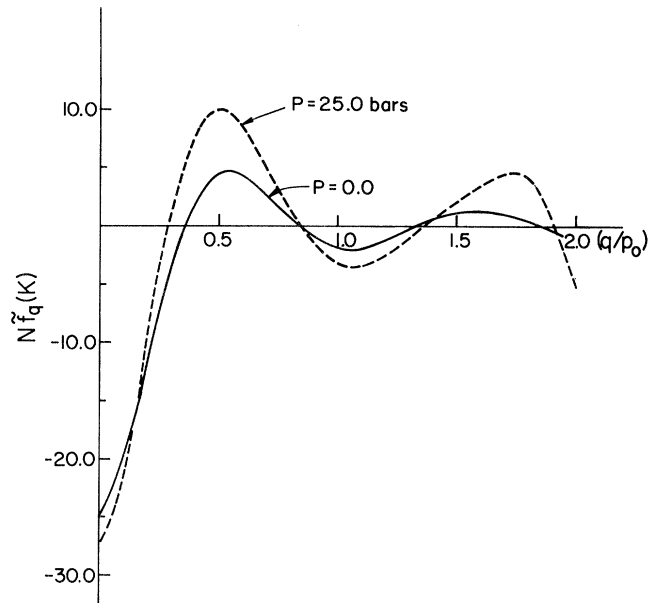


FIG. 11. Fourier transform of the roton pseudopotential for two pressures  $p=0.0$  and  $p=25.0$  bars. The  $q=0$  value of the potentials multiplied by the density,  $N\tilde{f}_0$ , is the same for all pressures above 5 bars, i.e.,  $N\tilde{f}_0 = -28.0$  K.

cantly probe the structure of the core. In the present problem however, we are interested in momenta up to  $2p_0 \approx 4 \text{\AA}^{-1}$ . These momenta certainly begin to probe the structure of  $f(r)$  at short distances. However, the contribution to the core to the Fourier transform  $f(q)$  is much smaller than that of the region outside the core. For  $P \approx 0.0$  the core region at  $|\vec{q}|=0$  is 12% of the tail region and is negligible for  $|\vec{q}| \approx 0.5p_0$ . At melting pressures it is about 30% when  $\vec{q}=0$  and becomes markedly smaller for  $|\vec{q}| \approx 0.5p_0$ . It is plausible then to assume that only the qualitative feature of a soft-core potential is necessary and that the detailed structure of the potential for  $r < r_c$  is not significant.

## V. BOUND STATES AND TRANSPORT PROPERTIES

Given  $\tilde{f}(r)$  and its Fourier transform  $\tilde{f}_q$ , it is straightforward to use the expressions given in the Appendix to calculate the moments of the irreducible interaction  $\tilde{\Gamma}$ , scattering amplitude  $\Gamma$ , bound-state energies for various  $l$  channels, roton-liquid parameters, and the roton lifetime (or what is equivalent, the viscosity). Our principal results are given in four tables and in different figures; we comment on these briefly.

In Table I we present our results for the pseudopotential parameter and bound-state energies at  $K=0$ . Inspection of Eq. (3.5) shows that for a channel in which  $\tilde{\Gamma} \equiv 2g_4^l$  is negative, the binding energy depends on only the parameters  $g_4^l$  (given in Table II), which characterize the expansion of the pseudopotential in spherical harmonics (A6). The pseudopotential was chosen so as to yield the experimental bound state in the  $l=2$  channel. Maximum bind-

TABLE I. Pseudopotential parameters and bound-state energies in different angular momentum channels at various pressures.

Pressure (bars)	Core height (K)	Core radius (Å)	$N\tilde{f}_0$ (K)	Bound-state energy for $K=0$ (K)			
				$l=2$	$l=4$	$l=6$	$l=8$
0.0	1.48	3.307	-25.0	0.27 Experimental $0.27 \pm 0.04$	0.65	1.46	0.21
5.0	3.82	3.12	-27.5	No bound state	1.86	1.80	0.24
15.0	5.66	3.06	-28.0	No bound state	1.97	1.89	0.28
25.0	6.30	3.06	-28.0	No bound state	1.58	1.80	0.31

ing is achieved in the  $l=6$  channel because it is this spherical harmonic which is most out of phase with  $\tilde{f}_q$ , in such a way as to minimize the contribution made by the repulsive part of  $\tilde{f}_q$  (in momentum space) and to take maximum advantage of the attractive portion of this pseudopotential, as shown in Fig. 12. There is no binding in the  $l=0$  channel because the moment of  $\tilde{f}_q$  that contributes to  $g_4^0$  is positive. That there must exist substantial binding in partial waves higher than  $l > 4$  was known already from the work of Fomin,<sup>26</sup> Pitaevskii,<sup>27</sup> and Tüttö and Zawadowski<sup>29</sup>; we see that our pseudopotential has this desired property. Our results are consistent with the kinematic sum rule, (A9), which relates the spatial average of the roton pseudopotential to a sum over  $g_4^l$ . We find that partial waves higher than  $l=2$  contribute a substantial fraction ( $\sim 97\%$ ) of this sum rule (which has contributions from both even and odd spherical harmonics).

Given the quantities  $g_4^l$ , it is straightforward to calculate the azimuthal moments of the pseudopotential,  $g_4^m(K) \equiv \tilde{\Gamma}_m(K)/2$ , from Eq. (A11). A given moment  $g_4^m(K)$  contains contribution from both even and odd  $g_l$ 's. We list in Table II moments up to  $m=8$ . We call the attention of the reader to the very considerable amount of pair momentum structure present in each  $m$  channel, as displayed in Figs. 13(a)–(13d) for moments up to  $m=6$ . The structure again reflects the structure present in our pseudopotential. The major contributions to the viscosity (or what is equivalent, the roton lifetime) come from the various  $m$  channels for  $p_0 \lesssim K \lesssim 2p_0$ .<sup>23,24</sup> It is interesting to compare our calculated values of  $g_4^m$  with Tüttö's estimates of the channels and coupling required to obtain

agreement with experiment; the latter are displayed as the shadowed region of Fig. 2. The  $m=0$  channel is of particular importance because it determines the upper branch in neutron scattering experiments. We discuss it below; here we note only that in the immediate vicinity of  $K=2p_0$ ,  $g_4^0$  changes by an order of magnitude, since according to Eqs. (A9) and (A12a),  $g_4^0(2p_0) = \tilde{f}_0 \simeq -28 \times 10^{-38} \text{ erg cm}^{-3}$ , while  $g_4^0(1.95p_0) = -2.0 \times 10^{-38} \text{ erg cm}^{-3}$ . This rapid variation may be traced to the way in which the various  $P_l(\cos\theta_{13})$  contribute to  $g_4^0$  in the vicinity of  $2p_0$ . It comes about, in part, because we have put all rotons on the roton sphere; if this restriction is abandoned, we expect this structure to be smoothed out.

We note as well that our values for  $g_4^l$  are almost an order of magnitude smaller than those of  $g_4^m(K)$ , including  $g_4^m(K=0)$ . Thus the coupling measured in the light scattering experiments is almost an order of magnitude smaller than that which plays a significant role in determining the roton energy shift and lifetime. The quantity  $g_4^m(K=0)$  corresponds to an average of the roton pseudopotential in the equatorial region of the roton sphere (see Fig. 3), while the quantity  $g_4^l$  contains contributions from this pseudopotential which cover the entire roton sphere; the latter is therefore smaller than the former, because the "roton-sphere" contributions are, on average, both repulsive and attractive, and a considerable amount of cancellation takes place. For low pair momenta ( $K \ll p_0$ ), the latter average furnishes a more reliable estimate of the coupling strengths, because in practice rotons occupy a region  $\Delta p_0 \sim 0.2p_0$  around the roton sphere, and consequently the equatorial average does not provide an accu-

TABLE II. Calculated roton-roton coupling parameters at zero pressure. Results are presented both for different angular momenta at  $K=0$ , and for different azimuthal quantum numbers  $K \neq 0$ .

$m$ or $l$	$g_4^l$ ( $10^{-38} \text{ erg cm}^{-3}$ )	$g_4^m(K=0.0)$ ( $10^{-38} \text{ erg cm}^{-3}$ )	$g_4^m(K=0.5p_0)$ ( $10^{-38} \text{ erg cm}^{-3}$ )	$g_4^m(K=1.5p_0)$ ( $10^{-38} \text{ erg cm}^{-3}$ )
0	+0.077	-0.75	-0.68	-1.34
2	-0.106	-0.94	-0.89	-1.26
4	-0.165	-0.99	-1.08	-1.31
6	-0.247	-0.96	-0.93	-0.37
8	-0.094	-0.40	-0.36	-0.04

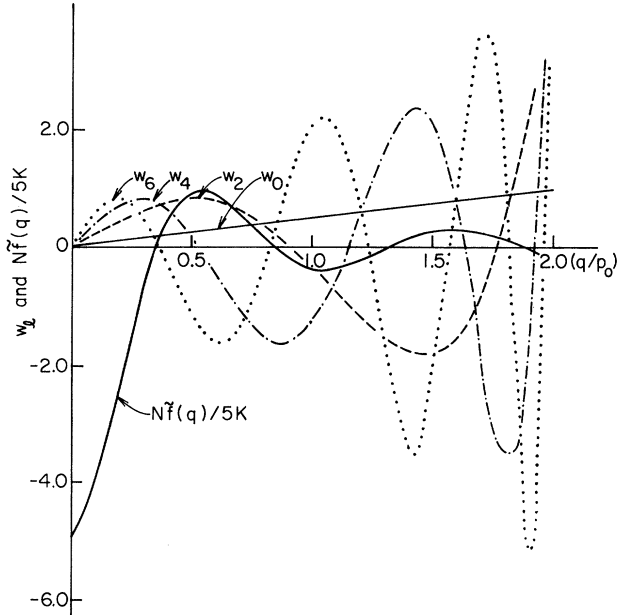


FIG. 12. Coupling constant  $g_4^l$  calculated as an integral over the product of the potential and a weight function [see Eq. (A3)]. In channel  $l$  the weight function with a suitable normalization is

$$w_l = \frac{2l+1}{2} \frac{q}{p_0} P_l \left[ 1 - \frac{q^2}{2p_0^2} \right].$$

The functions  $w_l$  for  $l=0,2,4,6$  are shown in order to compare with the Fourier transform of the pseudopotential  $\tilde{f}(q)$ . It can be clearly seen that the state  $l=6$  has the largest binding energy, since  $w_6$  is out of phase with  $N\tilde{f}(q)$  and, therefore,  $g_4^{l=6}$  is the most attractive coupling.

rate sampling of the momenta of importance in determining the roton-roton scattering amplitude.

We are thus led to the following picture:

(i) For large  $K$ ,  $p_0 \lesssim K \lesssim 2p_0$ , for example, the  $g_4^m$  provide an accurate estimate of the coupling strengths and can be used for calculating the roton-roton scattering amplitude and the existence of bound states.

(ii) At  $K=0$ , it is the quantities  $g_4^l$  that must be used to calculate scattering amplitudes and bound states.

(iii) As  $K$  increases from 0 to less than approximately  $p_0$  one crosses over from the  $g_4^l$ 's to the  $g_4^m$ 's; in the small- $K$  limit it likely suffices to use the most attractive  $g_4^l$  to estimate coupling strengths and calculate bound states, but in the crossover region detailed calculations must be carried out to determine the behavior of the bound states.

We use this picture to calculate the bound-state energies as a function of  $\vec{K}$ . In Fig. 14 we show for  $K=0$  the bound-state energies for various  $l$  channels calculated from Eq. (3.5) and, for  $p_0 \lesssim K \lesssim 2p_0$ , the bound-state energies for various  $m$  channels calculated from Eq. (3.9). Note that if one used the latter expression to calculate binding at  $K=0$ , one would obtain  $\epsilon_m(K=0) = -2x_c^2 \simeq -10$  K for all states, independent of coupling strength, a quite unphysical result. We note in Fig. 14 that the various calculated bound-state energies begin to become unphysical for  $K \sim p_0/2$ ; all of the various  $m$  channel energies have begun their precipitous descent to the limiting unphysical value of  $-10$  K.

We conclude that our results are reliable for  $K \gtrsim 1.5 \text{ \AA}^{-1}$ , and, for  $0.5 \lesssim K \lesssim 1.5 \text{ \AA}^{-1}$ , furnish a guide to interpolation of the kind pioneered by Pitaevskii and Fomin,<sup>27</sup> shown in Fig. 5. Since the lowest bound state at  $K=0$  occurs in the  $l=6$  channel, the bound-state energies of the azimuthal channels  $m=0, \pm 2, \pm 4, \pm 6$  must all terminate at this energy,  $E_b^{l=6} = 1.45$  K. (As Pitaevskii and Fomin<sup>27</sup> have shown, levels with the same  $m$  values which originate in different  $l$  values cannot cross.) One possible interpolation, consistent with these guidelines, is shown in Fig. 14. However, the possibility of local minima of the various bound-state energies at intermediate values of  $K$  cannot be ruled out.

Our results for the renormalized scattering amplitude, which determines in turn the roton energy shift and lifetime as well as the normal fluid density  $\rho_n$ , can be expressed in part through the roton-liquid parameters  $f_l$ . These are the moments of the renormalized amplitudes,  $\Gamma_m(K, E)$ , given by Eq. (3.20). The first four moments are displayed in Table III. An approximate sum rule for the

TABLE III. Calculated roton-liquid parameters at different pressures. In the last two lines of the table we compare our calculated values of the sum of the first four moments with the result predicted for all  $l$  by the approximate sum rule, Eq. (A17).

$l$	$Nf_l$ (K), $P=0.0$ bars	$Nf_l$ (K), $P=5.0$ bars	$Nf_l$ (K), $P=15.0$ bars	$Nf_l$ (K), $P=25.0$ bars
0	-9.78	-9.67	-9.18	-9.45
1	-0.81	-0.7	-1.05	-1.48
2	+9.5	+9.83	+12.47	+13.52
3	-0.93	-0.35	+2.31	+4.35
$\sum_{l=0}^3 Nf_l$	-2.02	-0.89	+4.55	+6.94
Approximate sum rule	2.73	3.17	3.78	4.28

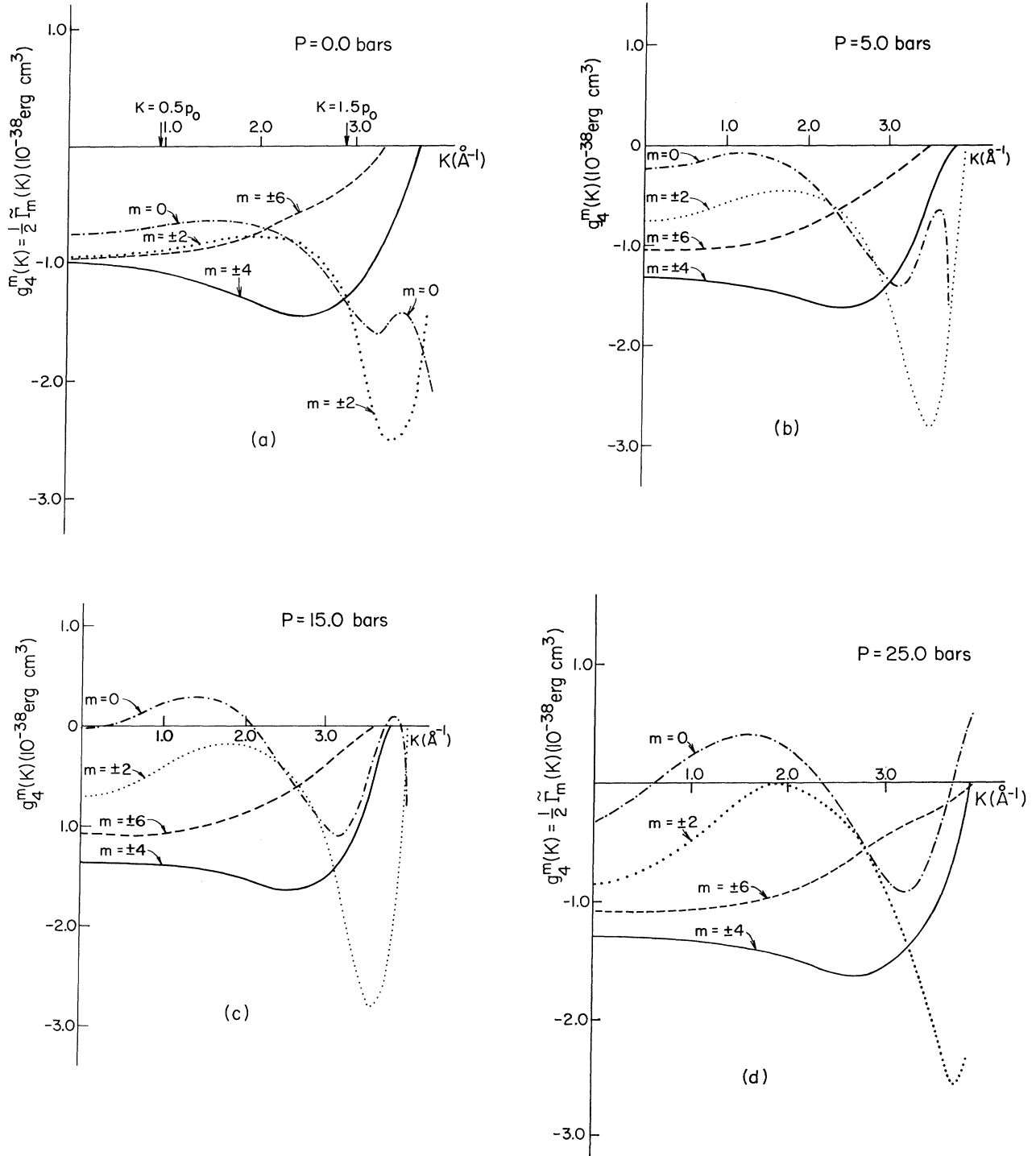


FIG. 13. Roton-roton interaction  $g_4^m(K)$  as a function of the total momentum  $K$  for different  $m$  channels at (a)  $p = 0.0$  bars, (b)  $p = 5.0$  bars, (c)  $p = 15.0$  bars, and (d)  $p = 25$  bars. The strength in the channel  $m = 0$  can be compared with the neutron scattering data (see Sec. VI). The plots are not continued to the vicinity of  $K = 2p_0$ , because the changes are very sharp. At  $K = 2p_0$ ,  $g_4^{m=0} = \tilde{f}_0$ , which has a value  $\tilde{f}_0 \approx -26$  K and  $g_4^m(2p_0) = 0$  for  $m \neq 0$ .

$f_l$  is derived in the Appendix [cf. Eq. (A17)]; we see on comparing the sum of the first four moments with  $\Gamma(2p_0)$  that significant contributions to the approximate sum rule must come from higher-order moments.

In Table IV we compare with experiment our calculated

values of the roton-liquid parameters,  $f_0$  and  $f_1$ , and the viscosity,  $\eta$ . The most recent measurement of the roton contribution to the viscosity is that of Len and Fozzoni,<sup>43</sup> who obtain good agreement with the results of previous workers.<sup>44</sup> Our pseudopotential  $\tilde{f}(r)$  was chosen so as to

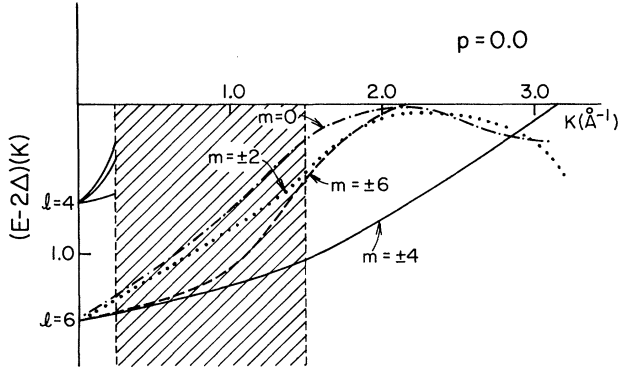


FIG. 14. Two-roton binding energy as a function of the total momentum in different  $m$  channels. The plotted values for  $K > 1.5 \text{ \AA}^{-1}$  are calculated from Eq. (3.9) with the cutoff defined in the text  $x_c^2 = \Delta_1 - \Delta$ . The splitting at small  $K$  is calculated using the formula of Pitaevskii and Fomin (Ref. 27), which contains a single parameter, the roton mass  $\mu$ . In the intermediate-momentum region (shaded area) no analytic expression is available; therefore the curves of small and large  $K$  are connected with smooth lines.

obtain good agreement with  $f_0$ , which in turn determines the shift with temperature of the roton energy. On the other hand,  $f_1$  and  $\eta$  are “derived” quantities. The agreement between theory and experiment for  $f_1$ , which measures “roton-liquid” corrections to the normal fluid density, and with the viscosity is seen to be quite good.

In Figs. 15(a) and 15(b) we present our results for the roton energy and lifetime as a function of temperature. The solid lines represent our theoretical calculations, which use the roton number given by Eq. (3.14), our adopted values of  $f_0$ , and our calculated value of the contribution made by our scattering amplitude to  $\Gamma_r$ . Analytic expressions for these quantities are

$$\Delta_0 - \Delta(T) = 24.72(1 + 0.0603T^{1/2})T^{1/2}e^{-\Delta(T)/T}, \quad (5.1)$$

$$\frac{\Gamma_r}{2} = 41.6(1 + 0.0603T^{1/2})T^{1/2}e^{-\Delta(T)/T}. \quad (5.2)$$

The good agreement with experiment for the roton energy is to be expected, since we have chosen our pseudopotential in such a way as to mimic the value of  $f_0$  used to determine this shift. On the other hand, like the viscosity, the agreement between theory and experiment for the roton lifetime below 1.4 K and above 1.8 K is a clear mea-

sure of the success of the present theory. (Between 1.4 and 1.8 K, the viscosity is independent of temperature, so that by calculating the viscosity accurately in this temperature regime, we are guaranteed success in our calculation of the roton lifetime.<sup>40</sup>)

We turn now to the results of our calculations at finite pressures. Because light scattering experiments to determine the  $l=2$  bound-state energy (if any) have not been carried out, we cannot use the  $l=2$  bound-state energy as an input to our choice of pseudopotential. We therefore choose our pseudopotential parameters in such a way as to obtain agreement between our theoretical calculations and the experimental values of the viscosity and  $f_0$  as a function of pressure.

We permit both the range  $r_c$  and the core height to vary; we expect that as the pressure increases, the distance at which the roton pseudopotential becomes repulsive will likewise decrease, because the underlying quasiparticles have a larger effective mass and hence less zero-point energy. Moreover, we expect the core height  $a$  to increase as the radius  $r_c$  decreases, because the rotons must then sample more of the underlying short-range repulsion between  $^4\text{He}$  atoms. Our calculated pseudopotential at 25 atm is shown in Fig. 10, while the core height and radius we adopt at four different pressures, and the  $K=0$  bound-state energies are given in Table I.

Our results for  $g_4^l$  as a function of density are given in Fig. 16. We predict that no  $l=2$  bound state exists at pressures greater than approximately 5 bars, while the  $l=4$ ,  $l=6$ , and  $l=8$  bound states persist up to 25 bars. The  $l=4$  state possesses marginally greater binding than the  $l=6$  pair state at 15 atm. We expect the  $K$  dependence of these bound-state energies to be qualitatively similar to that depicted in Fig. 16.

In Figs. 17(a) and 17(b) the calculated temperature dependence of the roton energy and of roton lifetime is presented for  $p=24.26$  bars. The experimental points of Dietrich *et al.*<sup>40</sup> are above the calculated curves. By using roton liquid theory, Bedell, Pines, and Fomin<sup>14</sup> derived a stability condition for the normal fluid density, which provides the inequality

$$\Delta(T) > \Delta_0 - T, \quad (5.3)$$

where  $\Delta_0 = \Delta(T=0)$ . The upper limit for  $\Delta(T)$  is represented by dashed lines in Figs. 15(a) and 17(a). The results of Dietrich *et al.*<sup>40</sup> at high temperatures may be seen to violate this stability condition both for  $p=0$  and for  $p=24.26$  bars; further determination of  $\Delta$  in this diffi-

TABLE IV. Comparison of calculated and measured roton-liquid parameters and viscosity at different pressures.

Pressure (bars)	$Nf_0$ (K)		$Nf_1/3$ (K)		Viscosity ( $\mu$ poise)	
	Theory	Experiment	Theory	Experiment	Theory	Experiment
0.0	-9.78	-9.7	-0.27	-0.4	12.7	12.5±0.4
5.0	-9.67	-9.7	-0.23	-0.33	14.3	13.8±0.4
15.0	-9.18	-9.0	-0.35	-0.33	17.1	16.5±0.4
25.0	-9.45	-9.5	-0.49	-0.8	19.1	18.7±0.4

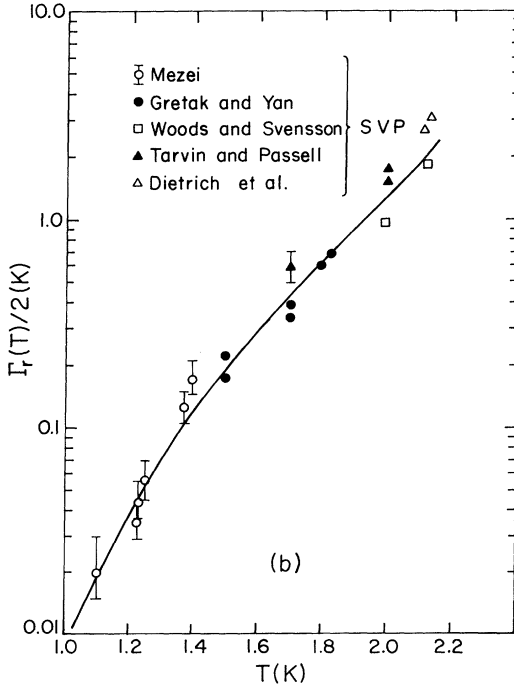
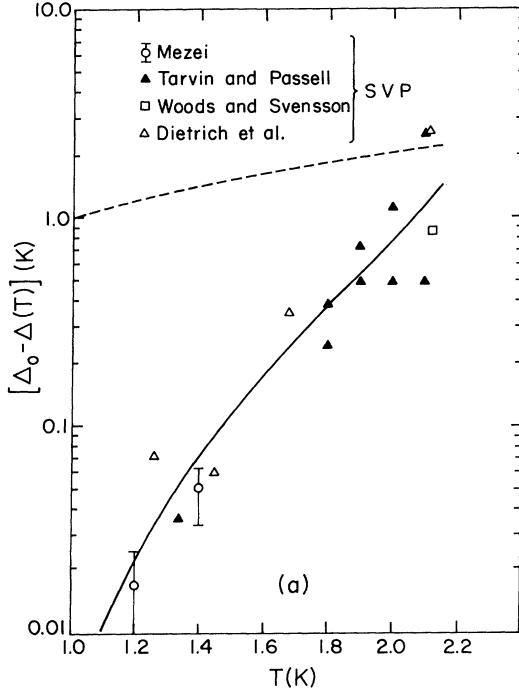


FIG. 15. Calculated roton parameters as a function of temperature at SVP  $p=0.0$  bars. (a) The calculated roton energy shift  $\Delta_0 - \Delta(T)$ , where  $\Delta(T=0) = \Delta_0$ . The experimental points are taken from Refs. 13, 40, 45, and 46, respectively. The dotted line represents the stability condition derived by Bedell, Pines, and Fomin (Ref. 14), above which the roton liquid is unstable. (b) Calculated roton halfwidth. The experimental points are taken from Refs. 13, 8, 40, 45, and 46, respectively.

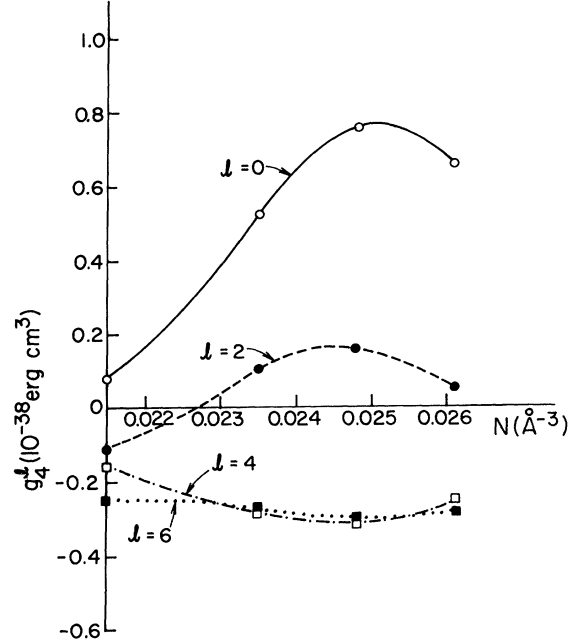


FIG. 16. Couplings  $g_4^l$  as a function of the density for different  $l$ .

cult (because of the large roton line width) temperature regime would seem highly desirable.

## VI. ROLE OF TWO-ROTON STATES IN NEUTRON SCATTERING

As we have remarked earlier, neutron scattering experiments provide a measure, through the dynamic factor, of the strength of the  $m=0$  component of the interaction of a pair of rotons of momentum  $\vec{K}$ . To the extent that the two-roton contribution can be regarded as distinct in energy from the other parts of the multiparticle branch, or from the single-particle branch, it may be written schematically in the form<sup>9</sup>

$$S^{(2)}(K, \omega) \propto \text{Im} \left[ \frac{F(K, \omega)}{1 - g_4^{\text{eff}}(K, \omega) F(K, \omega)} \right], \quad (6.1)$$

where  $F(K, \omega)$  describes the propagation of two noninteracting rotons, and  $g_4^{\text{eff}}(K, \omega)$  includes not only the direct roton-roton coupling we have considered in the preceding section, but an indirect term associated with the coupling of two-roton states to other components of the density-fluctuation excitation spectrum. These latter, hybridization, terms take the form, in second-order perturbation theory,<sup>24,29</sup>

$$g_4^{\text{ind}}(K) \simeq \frac{2g_3^2}{2\Delta - E(K)}, \quad (6.2)$$

where  $g_3$  is the strength of the vertex which couples the two-roton states to other excitations of momentum  $\vec{K}$ . The physical processes responsible for this indirect interaction are illustrated in Fig. 18. For low pair momenta, the excitations that couple most significantly to the two

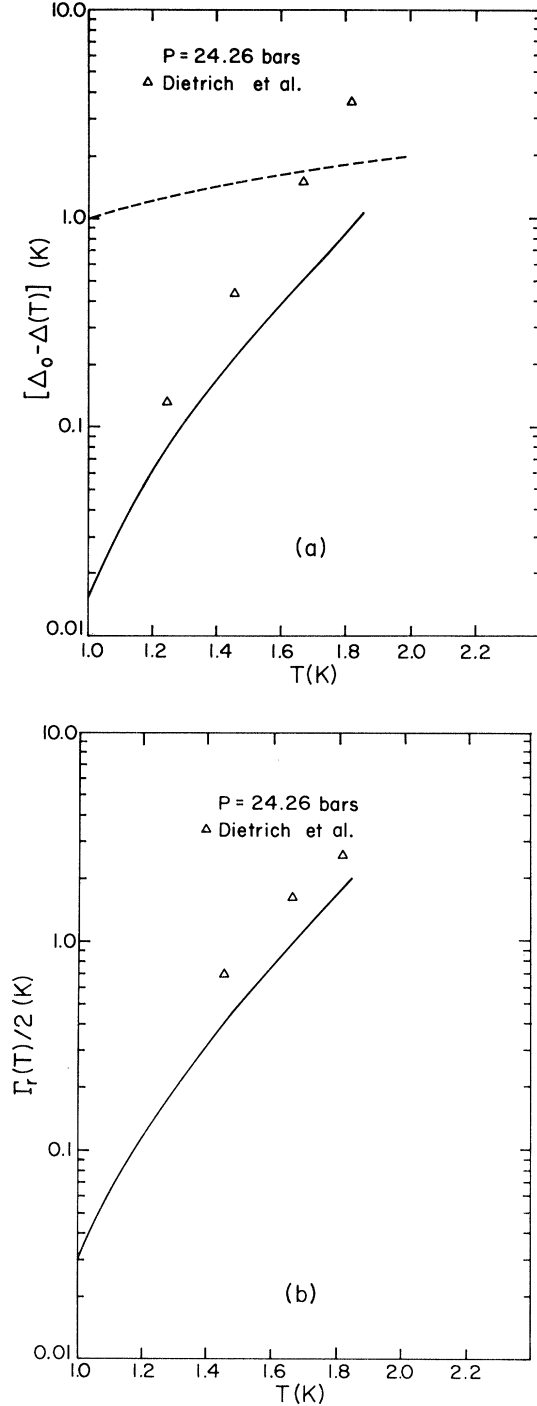


FIG. 17. Calculated roton parameters as a function of temperature at pressure  $p = 24.26$  bars. The plots are similar to Fig. 15. The experimental points are taken from Ref. 40.

roton state are the phonons of energy much less than  $2\Delta$ ; for large pair momenta ( $K \geq 3p_0/2$ ) the continuation of single-particle (phonon-maxon-roton) branch of the spectrum has negligible weight,<sup>9,27</sup> and it is the multiparticle excitations of energy  $E_K$  substantially higher than  $2\Delta$ , which couple most significantly to the two-roton state. The latter have an average energy close to  $K^2/2M$ , and a

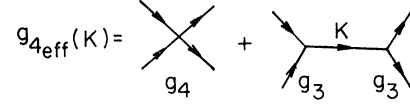


FIG. 18. Diagrammatic representation of the roton-roton coupling in the azimuthal channel  $m=0$ . The first term is the direct coupling between rotons and the second one is the coupling induced by an intermediate excitation of momentum  $K$ . The two-roton single-excitation coupling is labeled by  $g_3$ . It may be noted that the phonon-mediated coupling shown in Fig. 8 is incorporated in the direct coupling  $g_4$ .

very short lifetime against decay into yet more multiparticle excitations.

Thus we write

$$g_4^{\text{eff}}(K) = g_4^{m=0}(K) + g_4^{\text{ind}}(K), \quad (6.3)$$

where  $g_4^{m=0}(K)$  is the  $m=0$  component of our previously calculated direct interaction between rotons. We note that the  $g_3(q)$ , depicted in Fig. 14 as the vertex for the scattering of a roton from state  $\vec{p}_0$  to  $\vec{p}_0 + \vec{q}$ , accompanied by absorption of an excitation of momentum  $\vec{q}$  is identical to  $g_3$  considered above; however, the interaction  $g_4^{\text{ind}}(K)$  is *not* the phonon-induced interaction considered at the outset of Sec. IV (see Fig. 8) and which has already been incorporated into  $g_4^{m=0}(K)$ ; in the present “indirect” interaction, the intermediate states contain only a single excitation of momentum  $\vec{K}$ , energy  $E_K$ , while in the former, intermediate states contain three excitations. We further note that the additional coupling described by Eq. (6.2) is present only in the  $m=0$  channel; consequently, our calculations of transport properties and energy shift would require only slight modification, since these latter properties depend on a large number of  $m$  channels, many of which, in fact, turn out to be large compared to the  $m=0$  component.

As is evident from the above discussion, the sign of  $g_4^{\text{ind}}(K)$  depends on whether the excitations  $E_K$  of importance possess an energy that is greater or less than  $2\Delta$ . We consider the two possibilities separately, and further confine our remarks to these momenta which have been studied in some detail experimentally.

#### A. $2.7 \leq K \leq 3.3 \text{ \AA}^{-1}$

Here, as we have remarked,  $E(K) \gg 2\Delta$ , so that  $g_4^{\text{ind}} \leq 0$ . As Tüttö and Zawadowski<sup>29</sup> have emphasized, one cannot determine  $g_4^{\text{ind}}$  and  $g_4^{m=0}(K)$  separately from neutron scattering; however, from a fit to experiment based on (6.1), it is possible to deduce  $g_4^{\text{eff}}$ . Then, to the extent one has an independent knowledge of  $g_4^{m=0}(K)$ , one can infer  $g_4^{\text{ind}}$ , and hence  $g_3$  from experiment. We give in Table V values of  $g_4^{\text{eff}}(K)$  that we have calculated from the fit made by Smith *et al.*<sup>28</sup> to their experimental results. [Smith *et al.* did not, in fact, fit  $g_4^{\text{eff}}(K)$  directly, but list values of  $g_3$ ,  $g_4^{m=0}(K)$ , and  $E_K$  which fit their data, from

TABLE V. Coupling constants as a function of pair momentum and pressure.  $g_4^{\text{eff}}$  is obtained from neutron scattering experiments of Smith *et al.* (Ref. 28) [we have used the results given in A. J. Smith, Ph.D. thesis, University of Edinburgh, 1977 (unpublished)], as described in the text.  $g_4^m$  is taken from Fig. 13; the difference  $g_4^{\text{ind}} \equiv g_4^{\text{eff}} - g_4^{m=0}$  may originate in coupling induced by hybridization.

Pressure (bars)	Couplings ( $10^{-38}$ erg cm $^{-3/2}$ )	Pair momenta ( $\text{\AA}^{-1}$ )			
		2.7	2.9	3.1	3.3
1	$g_4^{\text{eff}}$	-1.85	-1.75	-1.5	-1.75
1	$g_4^{m=0}$	-1.05	-1.4	-1.5	-1.56
1	$g_4^{\text{ind}}$	-0.80	-0.35	0	-0.19
15	$g_4^{\text{eff}}$	-1.15	-1.3	-0.86	
15	$g_4^{m=0}$	-0.70	-0.90	-1.05	
15	$g_4^{\text{ind}}$	-0.45	-0.40	+0.19	
24.2	$g_4^{\text{eff}}$	-1.8	-1.15	-1.16	-1.39
24.2	$g_4^{m=0}$	-0.4	-0.7	-0.90	-0.90
24.2	$g_4^{\text{ind}}$	-1.4	-0.45	-0.26	-0.49
Error bars	>0.4 indicated in Ref. 28	>0.6	>0.7	>0.7	

which values we computed  $g_4^{\text{eff}}(K)$  using Eq. (6.3).] We also list in Table V our values of  $g_4^{m=0}(K)$  calculated using our pseudopotential, and the value of  $g_4^{\text{ind}}$  which we are able thereby to infer from Eq. (6.3).

We note that the values we obtain for  $g_4^{\text{ind}}$  in this way are negative (except for  $K=3.1 \text{ \AA}^{-1}$  at 15 atm) as is required since  $E_K > 2\Delta$  throughout this regime. Thus within the rather substantial uncertainties in the coupling strengths given in Ref. 28 ( $\Delta g \sim \pm 0.4$ ), our calculated values of  $g_4^{m=0}(K)$  are consistent with the results of the neutron scattering experiments. We further remark that the deduced decrease of  $g_4^{\text{ind}}$  (found at all pressures) with increasing pair momentum is likewise in accord with our theoretical expectations; as  $K$  increases from 2.7 to 3.3  $\text{\AA}^{-1}$  the mean multipair energy (with which we may expect  $E_K$  to scale) increases by a factor of 2; thus if  $E_K \sim 4\Delta$  at  $K=2.7 \text{ \AA}^{-1}$  and  $\sim 8\Delta$  at  $K \sim 3.3 \text{ \AA}^{-1}$ , one would have a change in  $g_4^{\text{ind}}(K)$  of the correct order of magnitude.

### B. $K=0.3 \text{ \AA}^{-1}$

Woods *et al.*<sup>47</sup> have measured the neutron spectrum at  $K=0.3 \text{ \AA}^{-1}$  with great accuracy; they find it exhibits two well-separated peaks corresponding to the single-excitation spectrum at energy 5 K and the two-roton resonance at  $\sim 2\Delta$ . The spectrum has been fitted by Ruvalds and Zawadowski,<sup>48</sup> using the formalism of Ruvalds *et al.*<sup>9,12</sup> From their results we extract a value of  $g_{\text{eff}} \cong 0.06 \pm 0.03 \times 10^{-38}$  erg cm $^3$ , a result which is an order of magnitude smaller than the effective couplings found at the larger momenta considered above. We further note that in this momentum region,  $2\Delta - E_K > 0$ , and hence  $g_4^{\text{ind}}$  must be positive; hence the direct interaction,  $g_4^{m=0}(K)$  must be negative, and  $|g_4^{m=0}| > |g_{\text{eff}}|$ .

Our theoretical calculations (see Fig. 13) do not, however, provide a reliable guide to the magnitude of  $g_4^{m=0}(K)$  for  $K \cong 0.3 \text{ \AA}^{-1}$ . The reason is that discussed in the

preceding section, namely, that for small momenta one wishes to average the pseudopotential over the equatorial region rather than the entire roton sphere; our theoretical calculations of  $g_4^{m=0}(K)$  at finite  $K$ , however, involve the latter averaging process and hence likely yield a considerable overestimate of  $g_4^{m=0}$ . We anticipate that more accurate calculations will yield results for both  $g_4^{m=0}$  and  $g_4^{\text{ind}}$  which are an order of magnitude smaller than their higher  $\bar{K}$  counterparts, i.e., results which typically are  $\sim 10^{-39}$  erg cm $^3$  rather than  $10^{-38}$  erg cm $^3$ . In other words, we anticipate that these quantities will be of the same order of magnitude as our calculated values of  $g_l$ . We also note that according to Fig. 14, for small values of  $\bar{K}$ , several different bound states, each characterized by the same azimuthal quantum  $m$ , are to be expected. The consequences of this degeneracy for a neutron scattering experiment remain to be explored.

In conclusion we note that our calculations predict a two-roton  $m=0$  bound state (arising solely as a consequence of the direct interaction) for the pair momentum region  $1.5 \leq K \leq 3 \text{ \AA}^{-1}$ ; as of this writing it has not proved possible to separate such a state from the broad multiparticle continuum. Indeed, for  $K \leq 2.7 \text{ \AA}^{-1}$ , although experimental measurements exist,<sup>47,49</sup> no theoretical fit to the data which takes into account both the two-roton component of the multiparticle branch of the excitation spectrum and the single-excitation branch has been carried out, apart from the fit made by Smith *et al.* for  $K=1.1 \text{ \AA}^{-1}$  at pressures of 19 and 25 atm.<sup>28</sup> We further call the attention of the reader (and the experimental community) to the prediction of our theory that, in contrast to our SVP results, at 25 atm the direct coupling,  $g_4^{m=0}(K)$  is positive for  $1 \leq K \leq 2.3 \text{ \AA}^{-1}$ , so that no two-roton bound states are to be expected. The above-mentioned fits at  $K=1.1 \text{ \AA}^{-1}$  in Ref. 28 for pressures of 19 and 25 atm yield a repulsive coupling  $g_4^{m=0} \approx 1.6 \times 10^{-38}$  erg cm $^3$ , which is larger than the value calculated by us. A more careful analysis of the data is required to draw a final conclusion, concerning the size of  $g_4^{m=0}$ .

## VII. DISCUSSION AND CONCLUSIONS

The pseudopotential we have proposed for the roton-roton interaction is a combination of a realistic He-He interaction at large distances and a short-range repulsive part. As a consequence it exhibits a relatively sharp attractive peak at a distance just beyond the onset, at  $r_c$ , of the repulsive part (see Fig. 10). It therefore resembles the phenomenological potential of Carballo and Ruvalds,<sup>30</sup> which was made up of two square wells, one repulsive, another attractive. They correctly realized that the attractive part must be comparatively long range in configuration space. The difference between their choice and ours comes primarily from the fact that our attractive potential, although long range, varies rapidly with increasing  $r$  for  $r > r_c$ , and hence exhibits sufficient structure to yield a considerable number of bound states with different symmetry.

Let us summarize briefly the main results of our calculations based on this pseudopotential:

(i) A substantial number of bound two-roton states of varying symmetry are found to exist for pair momenta up to  $K \sim 3 \text{ \AA}^{-1}$ .

(ii) The observed  $l=2$  bound state at  $K=0$  is correctly reproduced.

(iii) The effective roton coupling parameters at large momenta ( $K \sim p_0$ ) are an order of magnitude larger than those for  $K \ll p_0$ .

(iv) The calculated roton lifetime, roton contribution to the viscosity, and the temperature variation of the roton energy are in good agreement with experiment.

(v) The calculated roton-liquid parameters agree with those deduced from experiment by Bedell, Pines, and Fomin.<sup>14</sup>

(vi) By combining our theoretical results for the roton scattering amplitude at  $K \gtrsim p_0$  with the coupling parameters deduced from neutron scattering experiments, we obtain results for the phonon-mediated roton-roton interaction (in the  $m=0$  state) that are consistent with previous estimates based on mode-mode coupling theories.

Further experimental work which would test specific predictions of our theory include the following:

(i) A Raman scattering search for the predicted disappearance of the  $l=2$ ,  $K=0$  bound pair state at higher pressure (cf. Fig. 16).

(ii) More accurate higher pressure neutron scattering measurements of the energy and lifetime of rotons at temperatures greater than approximately 1.8 K, in order to resolve the present discrepancy between existing experiments and the limits on  $\Delta(T)$  placed by stability condition of roton-liquid theory<sup>14</sup> on the one hand, and roton-lifetime measurements on the other.

(iii) Careful neutron scattering measurements of the upper multiparticle branch of the spectrum for momenta  $\sim p_0/2$  to confirm our prediction that at pressures greater than approximately 15 bars the roton-roton coupling in this region will become repulsive. We note that the existing available data of Graf *et al.*<sup>49</sup> have not yet been analyzed from this point of view in sufficient detail to

provide a definitive answer to this question.

Moreover, more detailed neutron scattering experiments on the lifetime and shift with energy of the phonon-maxon-roton branch for momenta in the region  $p_0/3 \lesssim q \lesssim p_0$ , to study the interaction of these excitations with rotons, would provide insight into the extent to which our pseudopotential theory of interacting rotons can usefully be generalized to describe the interaction of phonons and maxons with rotons.

In the course of choosing our pseudopotential, and the calculations made with it, we have made certain approximations, the validity of which deserves further study:

(i) The repulsive part of our pseudopotential has been assumed to be independent of the pair momentum,  $K$ . Since it reflects a short-range scattering amplitude there is no *a priori* reason why this approximation, which led to a substantial reduction in the number of phenomenological parameters we need to introduce, is so successful.

(ii) We have ignored, or incorporated into our pseudopotential, via the short-range screening of the bare interaction, the interactions that are mediated by the exchange of other excitations. While we have been able to justify this approximation for small momentum transfers, the extent to which it is appropriate for large momentum transfers is less clear. The development of a better theory of hybridization, which should make possible a reliable estimate of the "three-excitation" vertex  $g_3$ , will be helpful in this connection.

(iii) In the density approach of Bogoliubov and Zubarev<sup>50,30</sup> vertex corrections occur which modify the roton-roton interaction by a factor which also depends only on the momentum transfer. Our attitude toward these corrections is that to the extent they play a role in our approach, they have likewise been incorporated in the short-range repulsive part of our pseudopotential.

(iv) We have used a momentum cutoff to restrict our treatment to excitations of momenta sufficiently near  $p_0$  that their dispersion can be described by a sum of quadratic and cubic terms.

(v) In order to simplify the treatment of the Bethe-Salpeter equation for finite pair momentum  $K$ , such information about the two-roton scattering amplitude along the ring region shown in Figs. 3 and 4 was incorporated in the irreducible interaction  $\tilde{\Gamma}$ . Thus  $\tilde{\Gamma}$  was assumed to depend only on the angle  $\phi$  also shown in Fig. 4. We have seen that this approximation is not appropriate for the momentum region  $0.5 < K < 1.5 \text{ \AA}^{-1}$ . Fortunately, this region carries a relatively small weight in our calculation of roton transport properties.

Future theoretical work which leads to a better solution of the Bethe-Salpeter equation for the two-roton scattering amplitude for pairs in the intermediate-momentum region ( $0.3 \lesssim K \lesssim 1.5 \text{ \AA}^{-1}$ ) would be highly desirable. It would also seem useful to develop a better theory of hybridization of the two-roton bound or resonant states with excitation of both lower and higher energy. We have begun such calculations using the polarization potential theory of Aldrich and Pines,<sup>16</sup> in which mode-mode coupling effects may be explicitly calculated, given a physical model for the coupled modes. Our goal is to calculate the

dynamic form factor measured in neutron scattering instead of the single-particle Green's function studied by Ruvalds *et al.*<sup>9,12</sup> Previous studies of the density-density correlation function<sup>16,51</sup> have not placed sufficient emphasis on roton-roton interactions to make possible a detailed comparison of theory and experiment for momentum regions in which its consequences are significant.

Finally we believe it will be fruitful to study maxon-maxon and maxon-roton interactions using the approach developed in this paper, by describing these interactions with a configuration-space pseudopotential of the same general character (but with a somewhat altered range and strength of the repulsive part) as that introduced here for roton-roton interactions and to extend our present approach to describe as well the interaction between phonons (i.e., excitations with momenta less than approximately  $0.9 \text{ \AA}^{-1}$ ) and thermally excited rotors. Work is underway along these lines as well.

#### ACKNOWLEDGMENTS

Part of this work has been done while we were participants in the Nordita-Landau Institute Research Group meeting at Göteborg, and part while we were participants in the summer program of the Aspen Center for Physics. It gives us pleasure to thank these organizations for their hospitality. One of us (A.Z.) would like to thank R. Orbach and T. Holstein and the Physics Department of the University of California at Los Angeles for their hospitality, where a portion of this work was carried out. This work was supported in part by National Science Foundation Grant No. DMR-82-15128 and U.S. Department of Energy Grant No. DE-AC02-76ER13001.

#### APPENDIX

We here show how the unrenormalized symmetrized vertex  $\tilde{\Gamma}(\vec{p}_1\vec{p}_2; \vec{p}_3\vec{p}_4)$ , which describes the roton-roton scattering, can be expressed in terms of various moments of the roton-roton pseudopotential  $\tilde{f}(r)$ . In addition we derive an approximate sum rule for the roton-liquid parameters  $f_l$ .

It is convenient to introduce relative momenta  $\vec{k} = \frac{1}{2}(\vec{p}_1 - \vec{p}_2)$  and  $\vec{k}' = \frac{1}{2}(\vec{p}_3 - \vec{p}_4)$ ; the momentum transfers in the interaction mediated by pseudopotentials are then

$$\vec{q} = \vec{k} - \vec{k}'$$

and

$$\vec{q}' = \vec{k} + \vec{k}' ,$$

while Eq. (4.6) takes the form

$$\begin{aligned} \tilde{\Gamma}(\vec{p}_1, \vec{p}_2; \vec{p}_3, \vec{p}_4) &= \tilde{\Gamma}(\vec{k}, \vec{k}'; \vec{K}) \\ &= \tilde{f}_{|\vec{k} - \vec{k}'|} + \tilde{f}_{|\vec{k} + \vec{k}'|} . \end{aligned} \quad (\text{A1})$$

If we further restrict ourselves to the case of physical interest in which all four excitations are close to the roton sphere, i.e.,  $|\vec{p}_i| = p_0$ , for all four roton momenta, then  $\tilde{\Gamma}(\vec{p}_1, \vec{p}_2; \vec{p}_3, \vec{p}_4)$  depends only on the angles  $\theta_{13}$  and  $\theta_{14}$  be-

tween  $(\vec{p}_1, \vec{p}_3)$  and  $(\vec{p}_2, \vec{p}_4)$ , respectively, or what is equivalent, on the angles  $\theta$  and  $\phi$  shown in Fig. 4. We thus have

$$\begin{aligned} \tilde{\Gamma}(\vec{k}, \vec{k}'; \vec{K}) &= \tilde{\Gamma}(\theta, \phi) \\ &= \sum_l (2l+1) g_4^l [P_l(\cos\theta_{13}) + P_l(\cos\theta_{14})] , \end{aligned} \quad (\text{A2})$$

where

$$g_4^l = \frac{1}{2} \int_{-1}^1 d \cos\theta P_l(\cos\theta) \tilde{f}_q \quad (\text{A3})$$

and

$$q^2 = 2p_0^2(1 - \cos\theta_{13}) \quad (\text{A4})$$

and

$$q'^2 = 2p_0^2(1 - \cos\theta_{14}) .$$

The relationship between the variables  $\theta_{13}$  and  $\theta_{14}$ ,  $\theta$  and  $\phi$  is given by

$$\cos\theta_{13} = \frac{1}{2}(1 + \cos\theta) + \frac{1}{2}(1 - \cos\theta)\cos\phi , \quad (\text{A5a})$$

$$\cos\theta_{14} = \frac{1}{2}(1 + \cos\theta) - \frac{1}{2}(1 - \cos\theta)\cos\phi , \quad (\text{A5b})$$

or what is equivalent,

$$\cos\theta_{13} = (K/2p_0)^2 + [1 - (K/2p_0)^2]\cos\phi , \quad (\text{A5c})$$

$$\cos\theta_{14} = (K/2p_0)^2 - [1 - (K/2p_0)^2]\cos\phi , \quad (\text{A5d})$$

since the square of roton pair momentum,  $K^2 = |\vec{p}_1 + \vec{p}_2|^2 = 2p_0^2(1 + \cos\theta)$ . Under exchange  $\phi \rightarrow \phi + \pi$  and  $\cos\theta_{13} \leftrightarrow \cos\theta_{14}$ , Eq. (A2) is even.

The quantities  $g_4^l$  depend only on angular averages of the pseudopotential, which describe roton-roton interaction and provide the basic input into expressions for the roton-roton scattering amplitude and the physical quantities which depend upon it. We can rewrite our expression (A3) as

$$g_4^l = \frac{1}{2} \int_0^{2p_0} dq q \tilde{f}_q P_l \left[ 1 - \frac{q^2}{2p_0^2} \right] , \quad (\text{A6})$$

in which form one sees that the  $l$  dependence of  $g_4^l$  arises from different weightings of the pseudopotential  $\tilde{f}_q$  in  $q$  space via the geometric factor  $qP_l(1 - q^2/2p_0^2)$ . (See Fig. 12 for the  $q$  dependence of these weight factors.)

As discussed in Sec. II, light scattering experiments provide information on the  $K=0$  limit of the irreducible vertex, Eq. (A2). In this limit, one sees from Fig. 4 or Eq. (A5c) that  $\theta_{13} \rightarrow \phi$ . Hence on comparing the  $K=0$  limit of Eq. (A2) with our earlier result, Eq. (3.2a), we obtain

$$\tilde{\Gamma}_l = 2g_4^l \quad (\text{for even } l) . \quad (\text{A7})$$

In other words, in this limit the moments  $g_4^l$  are equivalent to the moments of the previously defined irreducible roton vertex, and thus determine the binding energy  $\epsilon_l$  of the two-roton bound state given in Eq. (3.5).

We can likewise obtain a simple expression for the spatial average of the roton pseudopotential  $\tilde{f}_0$  by taking the

inverse of Eq. (A3),

$$\tilde{f}_q = \sum_l (2l+1)g_4^l P_l(\cos\theta_{13}), \quad (\text{A8})$$

and passing to the  $q=0$  limit. Since in this limit  $\theta_{13}=0$ , Eq. (A8) then reduces to

$$\tilde{f}_0 = \sum_l (2l+1)g_4^l. \quad (\text{A9})$$

For finite  $K$  we expand  $\tilde{\Gamma}$  in the azimuthal angle [compare Eq. (3.6a)],

$$\tilde{\Gamma}(K, \phi) = \sum_{m(\text{even})} \tilde{\Gamma}_m(K) e^{im\phi}. \quad (\text{A10})$$

If we compare the inverse of this equation with Eq. (A2), we obtain (for even  $m$ ),

$$\begin{aligned} \tilde{\Gamma}_m(K) &= \sum_l (2l+1)g_4^l \int_0^{2\pi} \frac{d\phi}{2\pi} \cos(m\phi) \\ &\quad \times [P_l(\cos\theta_{13}) + P_l(\cos\theta_{14})] \\ &= 2 \sum_l (2l+1)g_4^l \int_0^{2\pi} \frac{d\phi}{2\pi} \cos(m\phi) P_l(\cos\theta_{13}). \end{aligned} \quad (\text{A11})$$

In the limit  $|\vec{K}| \rightarrow 2p_0$ , which may be seen from Eq. (A5c) to correspond to  $\cos\theta_{13}=1$ , we find

$$\tilde{\Gamma}_0(2p_0) = 2 \sum_l (2l+1)g_4^l \quad (\text{A12a})$$

and

$$\tilde{\Gamma}_m(2p_0) = 0 \quad \text{for } m \neq 0. \quad (\text{A12b})$$

For arbitrary values of  $K$ , the moment  $\tilde{\Gamma}_m(K)$  will have contributions from all of the moments  $g_4^l$  with  $l \geq m$ . In general we shall see that for smaller values of  $m$  there will be more structure in  $\tilde{\Gamma}_m(K)$ . [See Figs. 13(a) and 13(b).]

Finally we derive a sum rule for the parameters introduced by Bedell, Pines, and Fomin<sup>14</sup> in their roton-liquid theory. From the expansion of the renormalized vertex function  $\Gamma$  given by Eq. (3.6b) we find for the vertex  $\Gamma(\vec{p}, \vec{p}'; E)$  in Eq. (3.10)

$$\begin{aligned} \text{Re}\Gamma(\vec{p}, \vec{p}'; E=2\Delta+T) &= \sum_{m(\text{even})} \text{Re}[\Gamma_m(K, E=2\Delta+T)] \\ &= \sum_l f_l P_l \left[ \frac{\vec{p} \cdot \vec{p}'}{p_0^2} \right], \end{aligned} \quad (\text{A13})$$

where Eqs. (3.18) and (3.19) have been also taken into account. On the other hand, in the case of  $\theta=0$ ,  $\vec{p}=\vec{p}'$ ,  $K=2p_0$ , the scattering amplitude is independent of  $\phi$ ; thus in expansion (3.6b) only the  $m=0$  component is different from zero, and Eq. (A13) takes the simple form

$$\sum_l f_l = \text{Re}\Gamma_0(K=2p_0, E=2\Delta+T). \quad (\text{A14})$$

On making use of Eq. (3.11), we obtain

$$\begin{aligned} \text{Re}\Gamma_0(K=2p_0, E=2\Delta+T) &= \\ &\approx \frac{\frac{8\pi}{\mu p_0} \gamma_0(2p_0) \left[ 1 + \ln \left[ \frac{2x_c^2}{T} \right] \gamma_0(2p_0) \right]}{\pi^2 \gamma_0^2(2p_0) + \left[ 1 + \ln \left[ \frac{2x_c^2}{T} \right] \gamma_0(2p_0) \right]^2}, \end{aligned} \quad (\text{A15})$$

where

$$\gamma_0(2p_0) = \frac{\mu p_0}{8\pi} \tilde{\Gamma}_0(2p_0) = \frac{\mu p_0}{4\pi} \tilde{f}_0, \quad (\text{A16})$$

and  $T=1.4$  K as discussed in Sec. III.

If now we combine Eqs. (A14) and (A15), we obtain the sum rule

$$\sum_l N f_l = \frac{\left[ \frac{8\pi}{\mu p_0} N \left[ \gamma_0^{-1}(2p_0) + \ln \left[ \frac{2x_c^2}{\xi} \right] \right] \right]}{\pi^2 + \left[ \gamma_0^{-1}(2p_0) + \ln \left[ \frac{2x_c^2}{\xi} \right] \right]^2} \Bigg|_{\xi=1.4 \text{ K}} \quad (\text{A17})$$

It should be emphasized that Eq. (3.11) is not exact for  $K=2p_0$ , because in deriving it the expression  $\mu_0 p_0^2 / 4\pi K$  has been used for the two-roton density of states. As  $\omega$  becomes larger than  $2\Delta$  the correct density of state deviates from this result (see case C in the Appendix of Zawadowski *et al.*<sup>9</sup>) Consequently our result (A17) is slightly modified at  $K=2p_0$ , and the exact sum rule given by Eq. (A14) is only approximated by (A17). To the extent that (A17) is valid, we find in Sec. V that the roton-liquid parameters do not obey the sum rule (see Table III) because the convergence of  $\sum_l N f_l$  is very slow.

\*Present address.

†Permanent address: Central Research Institute for Physics, P.O. Box 49, H-1525 Budapest, Hungary.

<sup>1</sup>L. D. Landau, *J. Phys. (Moscow)* **5**, 71 (1941); **11**, 91 (1947).

<sup>2</sup>R. P. Feynman, *Phys. Rev.* **94**, 262 (1954); R. P. Feynman and M. Cohen, *ibid.* **102**, 1189 (1956).

<sup>3</sup>M. Cohen and R. P. Feynman, *Phys. Rev.* **107**, 13 (1957).

<sup>4</sup>See, e.g., A. D. B. Woods and R. A. Cowley, *Can. J. Phys.* **49**, 177 (1970) and references cited therein.

<sup>5</sup>See for review, R. A. Cowley, in *Quantum Liquids*, edited by J.

Ruvalds and T. Regge (North-Holland, Amsterdam, 1978), p. 27.

<sup>6</sup>See for review, W. G. Stirling, *J. Phys. Paris (Colloq.)* **39**, C6-1334 (1978).

<sup>7</sup>L. P. Pitaevskii, *Zh. Eksp. Teor. Fiz.* **36**, 1169 (1958) [*Sov. Phys.—JETP* **2**, 830 (1959)].

<sup>8</sup>T. J. Greytak and J. Yan, *Phys. Rev. Lett.* **22**, 987 (1969).

<sup>9</sup>J. Ruvalds and A. Zawadowski, *Phys. Rev. Lett.* **25**, 333 (1970); A. Zawadowski, J. Ruvalds, and J. Solana, *Phys. Rev. A* **5**, 399 (1972).

- <sup>10</sup>F. Iwamoto, *Prog. Theor. Phys.* **44**, 1135 (1970).
- <sup>11</sup>See for review T. J. Greytak, in *Quantum Liquids*, Ref. 5, p. 121.
- <sup>12</sup>See for review A. Zawadowski, in *Quantum Liquids*, Ref. 5, p. 293.
- <sup>13</sup>F. Mezei, *Phys. Rev. Lett.* **44**, 1601 (1980).
- <sup>14</sup>K. Bedell, D. Pines, and I. Fomin, *J. Low Temp. Phys.* **48**, 417 (1982).
- <sup>15</sup>D. Pines, in *Quantum Fluids, Proceedings of the Sussex University Symposium, August 1965*, edited by D. F. Brewer (North-Holland, Amsterdam, 1966), p. 257.
- <sup>16</sup>C. H. Aldrich III, and D. Pines, *J. Low Temp. Phys.* **25**, 677 (1976).
- <sup>17</sup>C. H. Aldrich III, C. J. Pethick, and D. Pines, *J. Low Temp. Phys.* **25**, 691 (1976).
- <sup>18</sup>C. H. Aldrich III, C. J. Pethick, and D. Pines, *Phys. Rev. Lett.* **37**, 845 (1976).
- <sup>19</sup>L. D. Landau and I. M. Khalatnikov, *Zh. Eksp. Teor. Fiz.* **19**, 637 (1949) [*Sov. Phys.—JETP* **12**, 216 (1948)].
- <sup>20</sup>A. D. B. Woods, P. A. Hilton, R. Scherm, and W. G. Stirling, *J. Phys. C* **10**, L45 (1977).
- <sup>21</sup>M. J. Stephens, *Phys. Rev.* **187**, 279 (1969).
- <sup>22</sup>J. Yau and M. J. Stephens, *Phys. Rev. Lett.* **27**, 482 (1971).
- <sup>23</sup>J. Solana, V. Celli, J. Ruvalds, I. Tüttő, and A. Zawadowski, *Phys. Rev. A* **6**, 1665 (1972).
- <sup>24</sup>I. Tüttő, *Low Temp. Phys.* **11**, 77 (1973).
- <sup>25</sup>K. Nagai, *Prog. Theor. Phys.* **49**, 46 (1973); K. Kebukawa, *ibid.* **39**, 388 (1973).
- <sup>26</sup>I. A. Fomin, *Zh. Eksp. Teor. Fiz.* **60**, 1178 (1971) [*Sov. Phys.—JETP* **33**, 637 (1971)].
- <sup>27</sup>L. P. Pitaevskii and I. A. Fomin, *Zh. Eksp. Teor. Fiz.* **65**, 2516 (1973) [*Sov. Phys.—JETP* **38**, 1257 (1974)].
- <sup>28</sup>A. J. Smith, R. A. Cowley, A. D. B. Woods, W. G. Stirling, and P. Martel, *J. Phys. C* **10**, 543 (1977).
- <sup>29</sup>I. Tüttő and A. Zawadowski, *J. Phys. C* **11**, 385 (1978).
- <sup>30</sup>J. A. Carbello and J. Ruvalds, *Phys. Rev. B* **11**, 4278 (1975).
- <sup>31</sup>A. K. Rajagopal, A. Bagchi, and J. Ruvalds, *Phys. Rev. A* **9**, 2707 (1974).
- <sup>32</sup>S. Yamasaki, T. Kebukawa, and S. Sunakawa, *Prog. Theor. Phys.* **54**, 348 (1975).
- <sup>33</sup>T. Nishiyama and S. Sai, *Prog. Theor. Phys.* **52**, 1784 (1974).
- <sup>34</sup>T. Sugiyama, *Prog. Theor. Phys.* **63**, 1170 (1980).
- <sup>35</sup>K. Fukushima, N. Koyoma, and T. Sugiyama, *Prog. Theor. Phys.* **61**, 367 (1979).
- <sup>36</sup>K. Ishikawa and K. Yamada, *Prog. Theor. Phys.* **52**, 777 (1974).
- <sup>37</sup>E. Feenberg, *Theory of Quantum Fluids* (Academic, New York, 1969). This method is systematically applied, e.g., by D. K. Lee, *Phys. Rev.* **162**, 134 (1967).
- <sup>38</sup>See, e.g., Ref. 32; further references can be found in Ref. 30.
- <sup>39</sup>P. H. Roberts and R. J. Donnelly, *J. Low Temp. Phys.* **15**, 1 (1974).
- <sup>40</sup>O. W. Dietrich, E. H. Graf, C. H. Huang, and L. Passell, *Phys. Rev. A* **15**, 1377 (1972).
- <sup>41</sup>R. A. Aziz, V. P. S. Nain, J. C. Carley, W. L. Taylor, and G. T. McConville, *J. Chem. Phys.* **70**, 4330 (1979).
- <sup>42</sup>Concerning the best experimental fit for the binding energy  $E_{l=2}=0.27$  K, see the review in Ref. 11. This estimation is based on the optical data in C. A. Murray, R. L. Woerner, and T. J. Greytak, *J. Phys. C* **8**, L90 (1975) and on the refined theory of Raman scattering given by R. L. Woerner and M. J. Stephens, *ibid.* **8**, L-464 (1975). In that theory, the decay of two rotons into two phonons is included. The best roton energy measured by neutrons is reported in Ref. 20.
- <sup>43</sup>M. J. Len and P. Fozzoni, *Phys. Lett.* **93A**, 91 (1982).
- <sup>44</sup>D. F. Brewer and D. O. Edwards, in *Proceedings of the 8th International Conference on Low Temperature Physics*, edited by R. O. Davies (Butterworths, London, 1963), p. 96; J. Wilks, *Liquid and Solid Helium* (Clarendon, Oxford, 1967), p. 72.
- <sup>45</sup>J. A. Tarvin and L. Passell, *Phys. Rev. B* **19**, 1458 (1979).
- <sup>46</sup>A. D. B. Woods and E. C. Svensson, *Phys. Rev. Lett.* **41**, 974 (1978).
- <sup>47</sup>A. D. B. Woods, E. C. Svensson, and P. Martel, *Neutron Inelastic Scattering, Grenoble* (International Atomic Energy Agency, Vienna, 1972), p. 359.
- <sup>48</sup>J. Ruvalds and A. Zawadowski (unpublished).
- <sup>49</sup>E. H. Graf, V. Y. Minkiewicz, H. Bjerrum Møller, and L. Passell, *Phys. Rev. A* **10**, 1748 (1974).
- <sup>50</sup>N. N. Bogoljubov and D. N. Zubarev, *Zh. Eksp. Teor. Fiz.* **28**, 129 (1958) [*Sov. Phys.—JETP* **1**, 83 (1955)].
- <sup>51</sup>W. Götze and M. Lücke, *Phys. Rev. B* **13**, 3825 (1976).